

## **Ternary recognition fluorescent probe for lysosome acidification counter-ion studies via Cl<sup>-</sup>, K<sup>+</sup>, and pH**

Guang-Yue Zou,<sup>a</sup> Fan Bi,<sup>a</sup> Shuai Chen,<sup>a, c</sup> Meng-Xian Liu\*,<sup>b</sup> and Yong-Liang Yu\*,<sup>a</sup>

<sup>a</sup> *Research Center for Analytical Sciences, Department of Chemistry, College of Sciences, Northeastern University, Box 332, Shenyang 110819, China*

<sup>b</sup> *Institute of Multidisciplinary Research for Advanced Materials, Tohoku University, 2-1-1 Katahira, Aoba-ku, Sendai 980-8577, Miyagi, Japan*

<sup>c</sup> *Foshan Graduate School of Innovation, Northeastern University, Foshan 528311, China*

### **Corresponding authors.**

\*Email: yuyl@mail.neu.edu.cn (Yong-Liang Yu); mengxian.liu.d5@tohoku.ac.jp

(Meng-Xian Liu)

Tel: +86 24 83688944; Fax: +86 24 83676698.

## **Electronic Supplementary Information**

## Materials

1-(3-dimethylaminopropyl)-3-ethylcarbodiimide hydrochloride (EDC HCl), cysteine, 1,6-hexamethylenediamine, N,N-diisopropylethylamine (DIPEA), and 3-aminophenol were purchased from Aladdin Chemistry Co., Ltd. (Shanghai, China, <https://www.aladdin-e.com/>).

3,4-Dihydroxy-5-nitrobenzaldehyde, dextran (MW 40000), 3-maleimidopropionic acid, ethyl 4-bromobutyrate, N-(2-aminoethyl)maleimide hydrochloride, 2,4-dimethylpyrrole, iodomethane, iodoethane, 9-acridinecarboxylic acid, and 3,5-dibromo-4-hydroxybenzaldehyde were purchased from Anhui Zesheng Technology Co., Ltd (Shanghai, China, <https://www.energy-chemical.com/front/index.htm>).

o-(7-azabenzotriazol-1-yl)-N,N,N',N'-tetramethyl uronium hexafluorophosphate (HATU) and pentaethylene glycol were purchased from Shanghai Bide Pharmaceutical Technology Co., Ltd (Shanghai, China, <https://www.bidepharm.com/>).

Tris(2-carboxyethyl)phosphine hydrochloride (TCEP), 2,2'-dinitro-5,5'-dithiodibenzoic acid (DTNB), trifluoroacetic acid (TFA), 4-dimethylaminopyridine (DMAP), 3,3' -dithiodipropionic acid, and chloranil were purchased from Macklin Reagent Co., Ltd. (Shanghai, China, <http://www.macklin.cn/>).

NaCl, NaOH, triethylamine (TEA), K<sub>2</sub>CO<sub>3</sub>, and KOH were purchased from Damao Chemical Reagent Factory (Tianjin, China, <http://www.dmreagent.com/>).

Tetrahydrofuran, ethanol, N,N-dimethylformamide (DMF), methanol (MeOH), dichloromethane (DCM), petroleum ether (PE), ethyl acetate (EA), acetonitrile, N,N-

dimethylacetamide (DMA), and propionic acid were purchased from Fuyu Chemical Co., Ltd (Dongying, China).

$\text{NaH}_2\text{PO}_4$ ,  $\text{Na}_2\text{HPO}_4$ , hydrochloric acid, p-toluenesulfonyl chloride, boron trifluoride diethyl etherate, and iron powder were purchased from Sinopharm Chemical Reagent Co., Ltd. (Shanghai, China, <https://www.sinoreagent.com/>).

Silica gel (200-300 mesh) was purchased from Qingdao Ocean Chemical Co., LTD. (Qingdao, China).

All of chemicals were used without further purification. Deionized (DI) water of 18 M $\Omega$  cm was used to prepare all aqueous solutions.

## **Apparatus and characterization**

NMR experiments were performed on a Bruker Avance NEO spectrometer. Photoluminescence spectra were obtained using a Shimadzu RF-6000 fluorescence spectrophotometer. MTT assay was conducted by using a BioTek Synergy H1 ELISA plate reader at 570 nm. Confocal laser scanning microscope (CLSM) images were obtained on an Olympus FV-1200 confocal laser scanning microscope.

## **Synthesis of Probe-CI**

**C11.** 9-Acridinecarboxylic acid (670 mg, 3 mmol), HATU (1901 mg, 5 mmol), and 780  $\mu\text{L}$  DIPEA were dispersed in 10 mL DMF. Then 1,6-hexamethylenediamine (1162 mg, 10 mmol) was added, and the mixture was stirred at room temperature for 3 h. Subsequently, 70 mL DCM was added and the mixture was washed with water ( $3 \times 50$  mL). The crude product was purified by silica gel column chromatography (DCM:MeOH:TEA = 100:10:1) to give pure C11 (711 mg, 77% yield).  $^1\text{H}$  NMR (500

MHz, DMSO-*d*6)  $\delta$  9.04 (t, *J* = 5.6 Hz, 1H), 8.21 (d, *J* = 8.7 Hz, 2H), 7.99 (d, *J* = 8.6 Hz, 2H), 7.90 (t, *J* = 7.5 Hz, 1H), 7.69 (t, *J* = 7.6 Hz, 2H), 3.51 (q, *J* = 6.6 Hz, 2H), 2.57 (t, *J* = 6.3 Hz, 2H), 1.72-1.62 (m, 2H), 1.48-1.33 (m, 6H), 1.07 (t, *J* = 7.0 Hz, 1H). <sup>13</sup>C NMR (126 MHz, DMSO-*d*6)  $\delta$  166.28, 143.02, 148.66, 131.07, 129.75, 127.15, 126.05, 122.24, 41.98, 39.60, 33.59, 29.51, 26.97, 26.58.

**Cl2.** Cl1 (643 mg, 2mmol) was dissolved in 20 mL acetonitrile, then HATU (925 mg, 3 mmol), 3-maleimidopropionic acid (507 mg, 3 mmol), and 780  $\mu$ L DIPEA were added. The mixture was stirred at room temperature for 2 h. The crude product was purified by silica gel column chromatography (EA:PE = 2:1) to give pure Cl2 (510 mg, 54% yield). <sup>1</sup>H NMR (500 MHz, DMSO-*d*6)  $\delta$  9.03 (t, *J* = 5.6 Hz, 1H), 8.20 (d, *J* = 8.8 Hz, 2H), 8.06-7.85 (m, 5H), 7.69 (t, *J* = 7.6 Hz, 2H), 7.02 (s, 2H), 3.62 (t, *J* = 7.3 Hz, 2H), 3.50 (q, *J* = 6.6 Hz, 2H), 3.03 (q, *J* = 6.5 Hz, 2H), 2.34 (t, *J* = 7.2 Hz, 2H), 1.66 (t, *J* = 7.4 Hz, 2H), 1.47-1.29 (m, 6H). <sup>13</sup>C NMR (126 MHz, DMSO-*d*6)  $\delta$  171.21, 169.61, 166.29, 148.66, 142.99, 135.02, 131.08, 129.74, 127.16, 126.05, 122.23, 39.59, 38.87, 34.64, 34.55, 29.49, 29.44, 26.75, 26.56.

**Probe-Cl.** Cl2 (473 mg, 1 mmol) was dissolved in 15 mL acetone, and 2 mL iodomethane was added. The mixture was refluxed at 65°C for 12 h. After cooling to room temperature, the precipitate was collected by filter and washed with DCM. After drying, pure Probe-Cl was obtained (132 mg, 27% yield). <sup>1</sup>H NMR (400 MHz, D<sub>2</sub>O)  $\delta$  8.24-8.07 (m, 6H), 7.83 (ddd, *J* = 8.9, 6.3, 1.6 Hz, 2H), 6.74 (s, 2H), 3.72-3.54 (m, 5H), 3.03 (t, *J* = 6.7 Hz, 2H), 2.38 (t, *J* = 6.4 Hz, 2H), 1.67 (p, *J* = 7.0 Hz, 2H), 1.38 (m, 4H), 1.30-1.22 (m, 3H). <sup>13</sup>C NMR (101 MHz, D<sub>2</sub>O)  $\delta$  173.13, 172.44, 165.68, 150.93,

139.71, 137.98, 134.40, 129.32, 126.10, 122.17, 119.79, 40.27, 39.23, 34.74, 34.56, 30.20, 28.08, 28.05, 25.87, 25.60.

### Synthesis of Probe-K

**K1.** p-toluenesulfonyl chloride (3813 mg, 20 mmol) was dissolved in 50 mL THF, then pentaethylene glycol (1906 mg, 8 mmol) and KOH (1683 mg, 30 mmol) were added. The mixture was stirred at room temperature for 24 h. After distilling off the solvent under reduced pressure, the residue was dissolved in 50 mL DCM, and washed by water ( $3 \times 50$  mL). After drying, pentaethylene glycol di(p-toluenesulfonate) was obtained and directly used for the next reaction. 3,4-dihydroxy-5-nitrobenzaldehyde (915.6 mg, 5 mmol) and  $K_2CO_3$  (3455.2 mg, 25 mmol) were dispersed in 50 mL DMF, and the mixture was heated at 80°C for 30 min. Then, pentaethylene glycol di(p-toluenesulfonate) (3006.6 mg, 5.5 mmol) was slowly added, and the mixture reacted under  $N_2$  at 80°C for 20 h. After cooling to room temperature, 100 mL DCM was added, and the mixture was washed by water ( $3 \times 100$  mL). The crude product was purified by silica gel column chromatography (DCM:MeOH = 15:1) to give pure K1 (554.9 mg, 18% yield).  $^1H$  NMR (400 MHz,  $CDCl_3$ )  $\delta$  9.90 (s, 1H), 7.83 (d,  $J = 1.8$  Hz, 1H), 7.61 (d,  $J = 1.8$  Hz, 1H), 4.52 (t,  $J = 5.0$  Hz, 2H), 4.28 (t,  $J = 4.6$  Hz, 2H), 3.95 (dt,  $J = 18.0, 5.0$  Hz, 4H), 3.77-3.61 (m, 14H).  $^{13}C$  NMR (101 MHz,  $CDCl_3$ )  $\delta$  188.95, 153.96, 147.37, 144.93, 131.23, 129.82, 127.98, 119.69, 114.37, 74.13, 71.03, 71.01, 70.90, 70.85, 70.54, 70.40, 69.97, 69.21, 69.19.

**K2.** K1 (385.4 mg, 1 mmol) was dissolved in 50 mL DCM, then 2,4-dimethylpyrrole (285.4 mg, 3 mmol) and 100  $\mu$ L TFA were added. The mixture was

stirred under N<sub>2</sub> at room temperature for 10 h. Subsequently, chloranil (245.9 mg, 1mmol) was added, and the mixture was continue stirred at room temperature for 45 min. Then, 4 mL boron trifluoride diethyl etherate and 3 mL TEA were added. After stirring at room temperature for 4 h, the mixture was washed by saturated salt water. The crude product was purified by silica gel column chromatography (DCM:MeOH = 100:1) to give pure K2 (181.0 mg, 30% yield). <sup>1</sup>H NMR (400 MHz, CDCl<sub>3</sub>) δ 7.31 (d, J = 1.9 Hz, 1H), 7.03 (d, J = 2.0 Hz, 1H), 6.02 (s, 2H), 4.48 (t, J = 5.0 Hz, 2H), 4.15 (t, J = 4.6 Hz, 2H), 3.95 (dt, J = 10.2, 4.9 Hz, 4H), 3.77-3.66 (m, 12H), 2.55 (s, 6H), 1.50 (s, 6H). <sup>13</sup>C NMR (101 MHz, CDCl<sub>3</sub>) δ 156.61, 154.39, 145.59, 142.70, 142.59, 137.95, 131.10, 130.42, 121.78, 116.81, 116.17, 74.17, 71.12, 71.11, 70.90, 70.79, 70.70, 70.41, 70.04, 70.02, 69.45, 69.28, 14.78.

**K3.** K2 (108.6 mg, 0.18 mmol) was dissolved in 30 mL ethanol, then iron powder (55.8 mg, 1 mmol), 700 μL 1 M hydrochloric acid and 1 mL water were added. The mixture was refluxed under N<sub>2</sub> at 80°C for 2 h. After distilling off the solvent under reduced pressure, 20 mL water was added, and extracted with ethyl acetate three times. The crude product was purified by silica gel column chromatography (DCM:MeOH = 15:1) to give pure K3 (82.6 mg, 80% yield).

**Probe-K.** 3-maleimidopropionic acid (33.6 mg, 0.2 mmol), HATU (76.0 mg, 0.2 mmol), and 139 μL DIPEA were dissolved in 20 mL acetonitrile, then K3 (57.3 mg, 0.1 mmol) was added. The mixture was stirred at room temperature for 30 min. The crude product was purified by silica gel column chromatography (DCM:MeOH = 15:1) to give pure Probe-K (54.3 mg, 75% yield). <sup>1</sup>H NMR (400 MHz, CDCl<sub>3</sub>) δ 8.54 (s, 1H),

7.92 (d,  $J = 1.8$  Hz, 1H), 6.69 (s, 2H), 6.57 (d,  $J = 1.9$  Hz, 1H), 5.96 (s, 2H), 4.46-4.36 (m, 2H), 4.20-4.12 (m, 2H), 3.96-3.86 (m, 4H), 3.84-3.76 (m, 4H), 3.69-3.54 (m, 10H), 2.70 (t,  $J = 7.3$  Hz, 2H), 2.54 (s, 6H), 1.53 (s, 6H).  $^{13}\text{C}$  NMR (101 MHz,  $\text{CDCl}_3$ )  $\delta$  170.40, 167.99, 155.34, 152.00, 143.09, 141.27, 131.55, 134.21, 133.34, 131.41, 130.16, 121.07, 112.82, 108.89, 74.24, 72.31, 70.79, 70.73, 70.60, 70.53, 70.22, 69.46, 68.69, 35.60, 33.98, 14.59, 14.52.

### Synthesis of Probe-pH

**pH1.** 3-aminophenol (1.31 g, 12 mmol), ethyl 4-bromobutyrate (2.34 g, 12 mmol), and DIPEA (2.09 mL, 12 mmol) were dissolved in 35 mL DMF, and the mixture was stirred at 100°C for 1.5 h. After cooling to room temperature, iodoethane (1.28 mL, 16 mmol) and DIPEA (2.09 mL, 12 mmol) were added, and the mixture was stirred at 80°C for 2 h. After cooling to room temperature, the reaction mixture was poured into 150 mL EA: PE 1:1 mixture, washed with water ( $2 \times 80$  mL). The organic phase was dried with anhydrous  $\text{Na}_2\text{SO}_4$ , and then the solvent was distilled off under reduced pressure. The crude product was purified by silica gel column chromatography (EA: PE = 1:4) to give pure pH1 (1.63 mg, 57% yield).  $^1\text{H}$  NMR (400 MHz,  $\text{CDCl}_3$ )  $\delta$  7.04 (t,  $J = 8.1$  Hz, 1H), 6.28-6.11 (m, 3H), 4.15 (q,  $J = 7.1$  Hz, 2H), 3.37-3.20 (m, 4H), 2.35 (t,  $J = 7.1$  Hz, 2H), 1.90 (p,  $J = 7.3$  Hz, 2H), 1.26 (t,  $J = 7.2$  Hz, 3H), 1.12 (t,  $J = 7.0$  Hz, 3H).  $^{13}\text{C}$  NMR (101 MHz,  $\text{CDCl}_3$ )  $\delta$  173.77, 157.04, 149.43, 130.13, 104.73, 102.89, 99.08, 60.67, 49.56, 45.10, 31.61, 22.75, 14.23, 12.28.

**pH2.** 3,5-dibromo-4-hydroxybenzaldehyde (0.70 g, 2.5 mmol), pH1 (1.26 g, 5.0 mmol), and p-toluenesulfonic acid (86 mg, 0.5 mmol) were dissolved in 42 mL

propionic acid, then the mixture was stirred at 80°C for 2 h. After cooling to room temperature, tetrachloro-1,4-benzoquinone (0.93 g, 3.8 mmol) was added and the mixture was stirred at room temperature for 12 h. After distilling off the solvent under reduced pressure, the crude product was purified by silica gel column chromatography (DCM: MeOH = 15:1) to give pure pH2 (0.97 g, 52% yield). <sup>1</sup>H NMR (400 MHz, CDCl<sub>3</sub>) δ 7.82 (d, J = 9.5 Hz, 2H), 7.56 (s, 2H), 6.93 (dd, J = 9.6, 2.5 Hz, 2H), 6.73 (d, J = 2.5 Hz, 2H), 4.20 (q, J = 7.1 Hz, 4H), 3.65-3.51 (m, 8H), 2.46 (t, J = 6.7 Hz, 4H), 2.02 (p, J = 6.9 Hz, 4H), 1.37-1.27 (m, 12H). <sup>13</sup>C NMR (101 MHz, CDCl<sub>3</sub>) δ 172.74, 157.62, 156.30, 154.45, 135.03, 133.34, 116.50, 114.45, 112.92, 112.39, 96.56, 60.86, 50.22, 46.11, 30.94, 22.48, 14.29, 12.51.

**Probe-pH.** pH2 (224 mg, 0.3 mmol) was dissolved in 20 mL methanol, and 2 mL 2 M KOH solution was added, and the mixture was stirred at room temperature for 5 h. The pH of the mixture was adjusted to neutral by hydrochloric acid. After distilling off solvent under reduced pressure, the residue was dissolved in 30 mL DMF. Then DIPEA (174 μL, 1.2 mmol), HATU (380 mg, 1.0 mmol), and aminoethyl maleimide hydrochloride (112 mg, 0.8 mmol) were added. The mixture was stirred at room temperature for 3 h. Subsequently, 100 mL water was added and extracted with DCM (3 × 50 mL). After distilling off the solvent under reduced pressure, the crude product was purified by silica gel column chromatography (DCM: MeOH = 15:1) to give pure Probe-pH (148.5 mg, 53% yield). <sup>1</sup>H NMR (400 MHz, CDCl<sub>3</sub>) δ 7.50 (s, 2H), 7.37 (d, J = 9.5 Hz, 2H), 6.98 (s, 4H), 6.69 (s, 4H), 3.78-3.52 (m, 16H), 2.38-2.26 (m, 4H), 2.08-1.96 (m, 4H), 1.34-1.28 (m, 6H). <sup>1</sup>H NMR (400 MHz, DMSO-*d*<sub>6</sub>) δ 8.00 (t, J = 4.0 Hz,



2H), 7.76 (s, 2H), 7.37 (d,  $J = 9.5$  Hz, 2H), 7.20 (d,  $J = 9.7$  Hz, 2H), 7.00 (s, 4H), 3.77-3.38 (m, 14H), 3.23 (d,  $J = 6.1$  Hz, 4H), 2.13 (t,  $J = 6.7$  Hz, 4H), 1.81 (t,  $J = 6.0$  Hz, 4H), 1.22 (t,  $J = 6.9$  Hz, 6H).  $^{13}\text{C}$  NMR (400 MHz, DMSO- $d_6$ )  $\delta$  171.69, 171.02, 157.34, 155.42, 134.49, 133.23, 131.56, 114.71, 112.99, 112.11, 96.22, 56.00, 45.79, 37.24, 36.95, 31.60, 18.52, 12.32.

### **Preparation of sulfhydryl-functionalized dextran (Dex-SH)**

Dextran (MW 40000, 1.63 g, 10 mmol measured as monomer) was dispersed in 10 mL DMA, and dissolved by heating. Then EDC HCl (6.17 g, 35 mmol), DMAP (0.86 g, 7 mmol), and 3,3' -dithiodipropionic acid (3.15 g, 15 mmol) were added, and the mixture was reacted at 60°C for 18 h. After adding 35 mL ethanol, the precipitation was collected by centrifugation and washed with ethanol ( $3 \times 10$  mL). After drying, 3,3' -dithiodipropionic acid modified dextran was obtained.

The above product (350 mg) was dissolved in 20 mM neutral phosphate buffer (PB), and added 750 mg TCEP. After stirring at room temperature for 12 h, the mixture was transferred to a dialysis bag (3000 Da) and dialyzed with deionized water for 36 h. After distilling off the solvent under reduced pressure, the residue was washed by ethyl acetate for 3 times. After drying, the Dex-SH was obtained.

### **Determination of sulfhydryl content in Dex-SH**

10.0 mg Dex-SH was dissolved in neutral PB, and diluted to 10 mL to obtain 1 mg mL<sup>-1</sup> stock solution. 9.9 mg DTNB was dissolved in neutral PB, and diluted to 25 mL to obtain 1 mM stock solution. 12.12 mg cysteine was dissolved in neutral PB, and diluted to 100 mL to obtain 1 mM stock solution. Sulfhydryl standard samples were

prepared by mixing DTNB with different concentrations of cysteine, where the concentration of DTNB was 100  $\mu\text{M}$  and the concentrations of cysteine were 0, 15, 30, 45, 75, and 90  $\mu\text{M}$ , respectively. The absorption spectra of the above solutions were measured after 1 h of standing and a standard curve was drawn based on the absorbance at 412 nm. The absorption spectra of mixtures of Dex-SH and DTNB were measured, and the sulfhydryl concentration and sulfhydryl content in Dex-SH were calculated according to the standard curve.

### **Preparation of ternary recognition fluorescent probe (TR-probe)**

The stock solutions of Probe-K (1 mM) and Probe-pH (1 mM) were prepared in DMF. The stock solutions of Probe-Cl (1 mM) and Dex-SH (1 mg mL<sup>-1</sup>) were prepared in neutral PB. 0.9 mL Probe-K stock solution, 3.5 mL Probe-pH stock solution, and 5 mL Probe-Cl stock solution were added to 5 mL Dex-SH stock solution, and the mixture was stirred at room temperature for 2 h. Then, the solution was transferred to a dialysis bag (3000 Da) and dialyzed with deionized water for 24 h. After drying, the solid was washed with ethyl acetate (3  $\times$  10 mL) and dried again to give the TR-probe.

### **Cell culture and MTT assay**

A549 cells were cultured in A549 special complete medium (purchased from Procell Life Science & Technology Co., Ltd) at 37°C under 5% CO<sub>2</sub>.

The viability of cells treated with TR-probe was determined by the MTT assay. A549 cells were cultured in a 96-well plate at 37°C under 5% CO<sub>2</sub> for 12 h. Then, cells were treated with different concentrations of TR-probe. After 24 h incubation, 20  $\mu\text{L}$  of 5 mg mL<sup>-1</sup> MTT solution was added into each well for 4 h. Then, the medium was

aspirated out, and 150  $\mu\text{L}$  of DMSO was added to dissolve the formazan. The absorbance at 570 nm was measured by a plate reader. Cell viability (%) was determined by the following equation: Viability = (mean Abs. of treated wells/mean Abs. of control wells)  $\times$  100%.

### **Colocalization experiment**

A549 cells were seeded in confocal dishes and incubated at 37°C under 5%  $\text{CO}_2$  for 12 h. Then, cells were incubated with 20  $\mu\text{g mL}^{-1}$  TR-probe for 8 h and 100 nM Lyso-Tracker DeepRed for 20 min. The images were obtained by an FV-1200 confocal laser scanning microscope with 60 $\times$  objective lens (cyan channel:  $\lambda_{\text{ex}}$  = 405 nm,  $\lambda_{\text{em}}$  = 460-500 nm; green channel:  $\lambda_{\text{ex}}$  = 488 nm,  $\lambda_{\text{em}}$  = 520-560 nm; red channel:  $\lambda_{\text{ex}}$  = 559 nm,  $\lambda_{\text{em}}$  = 575-625 nm; NIR channel  $\lambda_{\text{ex}}$  = 635 nm,  $\lambda_{\text{em}}$  = 655-755 nm). The colocalization analysis was performed by an FV10-ASW 4.2 software.

### **Imaging $\text{Cl}^-$ , $\text{K}^+$ , and pH in lysosomes**

The ions level in lysosomes was adjusted using previously published protocols [1-3]. A549 cells were seeded in confocal dishes and incubated at 37°C under 5%  $\text{CO}_2$  for 12 h. After that, cells were incubated with 20  $\mu\text{g mL}^{-1}$  TR-probe for 8 h. Then, the cells were washed and incubated in the clamping buffers used to regulate ion levels for 1 h at 25°C. The clamping buffers for adjusting  $\text{Cl}^-$  levels ( $[\text{Cl}^-]$  = 0, 5, 25, 125 mM) were prepared by a mixture chloride positive buffer (150 mM KCl, 20 mM NaCl, 1 mM  $\text{CaCl}_2$ , 1 mM  $\text{MgCl}_2$ , and 10 mM HEPES) to a chloride negative buffer (150 mM  $\text{KNO}_3$ , 20 mM  $\text{NaNO}_3$ , 1 mM  $\text{Ca}(\text{NO}_3)_2$ , 1 mM  $\text{Mg}(\text{NO}_3)_2$ , and 10 mM HEPES). The  $\text{Cl}^-$  clamping buffer also contained 50  $\mu\text{M}$  nigericin, 50  $\mu\text{M}$  monensin, and 25  $\mu\text{M}$

tributyltin chloride. The clamping buffers for adjusting  $K^+$  levels ( $[K^+] = 0, 50, 100, 150$  mM) were prepared by a mixture potassium positive buffer (150 mM KCl, 20 mM NaCl, 1 mM  $CaCl_2$ , 1 mM  $MgCl_2$ , and 10 mM HEPES) to a potassium negative buffer (170 mM NaCl, 1 mM  $CaCl_2$ , 1 mM  $MgCl_2$ , and 10 mM HEPES) to make  $[K^+] = 0, 50, 100, 150$  mM. The  $K^+$  clamping buffers also contained 50  $\mu$ M nigericin and 50  $\mu$ M monensin. The clamping buffers for adjusting pH contained 50  $\mu$ M nigericin 150 mM KCl, 20 mM NaCl, 1 mM  $CaCl_2$ , 1 mM  $MgCl_2$ , 1 mM  $NaH_2PO_4$ , and 10 mM HEPES at different pH (pH = 4, 5, 6, 7).

The images were obtained by an FV-1200 confocal laser scanning microscope with 60 $\times$ objective lens (cyan channel:  $\lambda_{ex} = 405$  nm,  $\lambda_{em} = 460$ -500 nm; green channel:  $\lambda_{ex} = 488$  nm,  $\lambda_{em} = 520$ -560 nm; red channel:  $\lambda_{ex} = 559$  nm,  $\lambda_{em} = 575$ -675 nm). The fluorescence optical density was calculated by image J software.

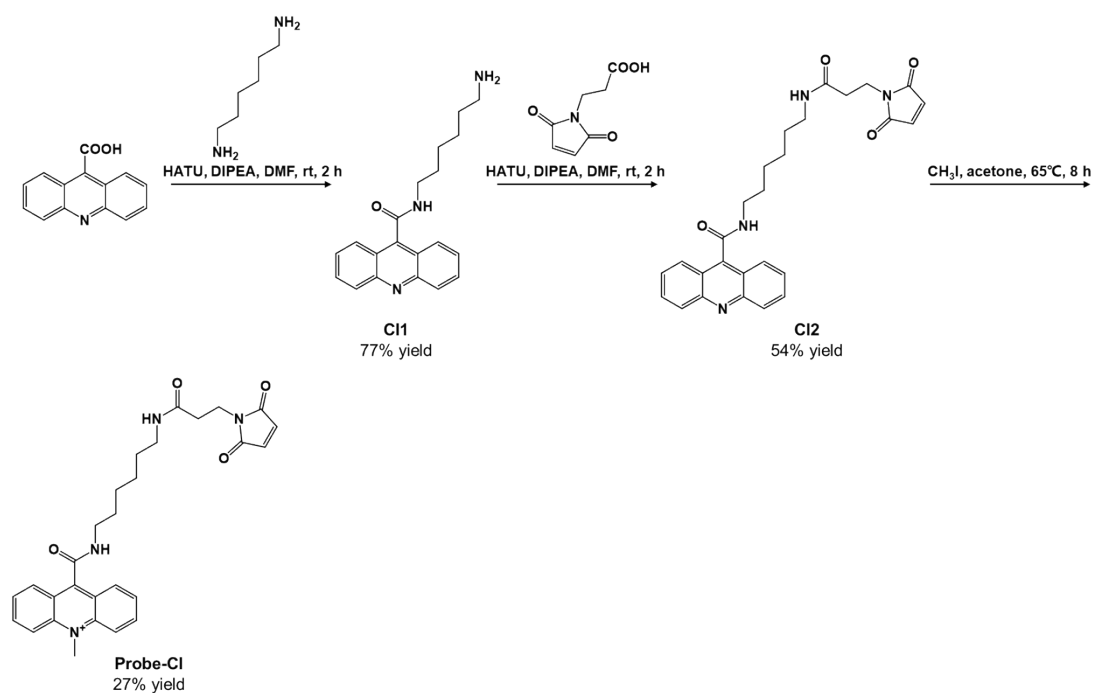
### **Imaging $Cl^-$ , $K^+$ , and pH in lysosomes under addition of KCl, $Cl^-$ channel inhibition, and oxidative stress**

A549 cells were seeded in confocal dishes and incubated at 37°C under 5%  $CO_2$  for 12 h. After that, cells were incubated with 20  $\mu$ g  $mL^{-1}$  TR-probe for 8 h. For KCl incubation experiment, cells were incubated in medium with additional KCl (200 mM) for 3 h. For  $Cl^-$  channel inhibition experiment, cells were incubated with chloride channel blocker NPPB (40  $\mu$ M) for 30 min. For oxidative stress experiment, cells were incubated with 0.2 mM  $H_2O_2$  for 1 h or 10  $\mu$ g  $mL^{-1}$  LPS for 4 h, respectively.

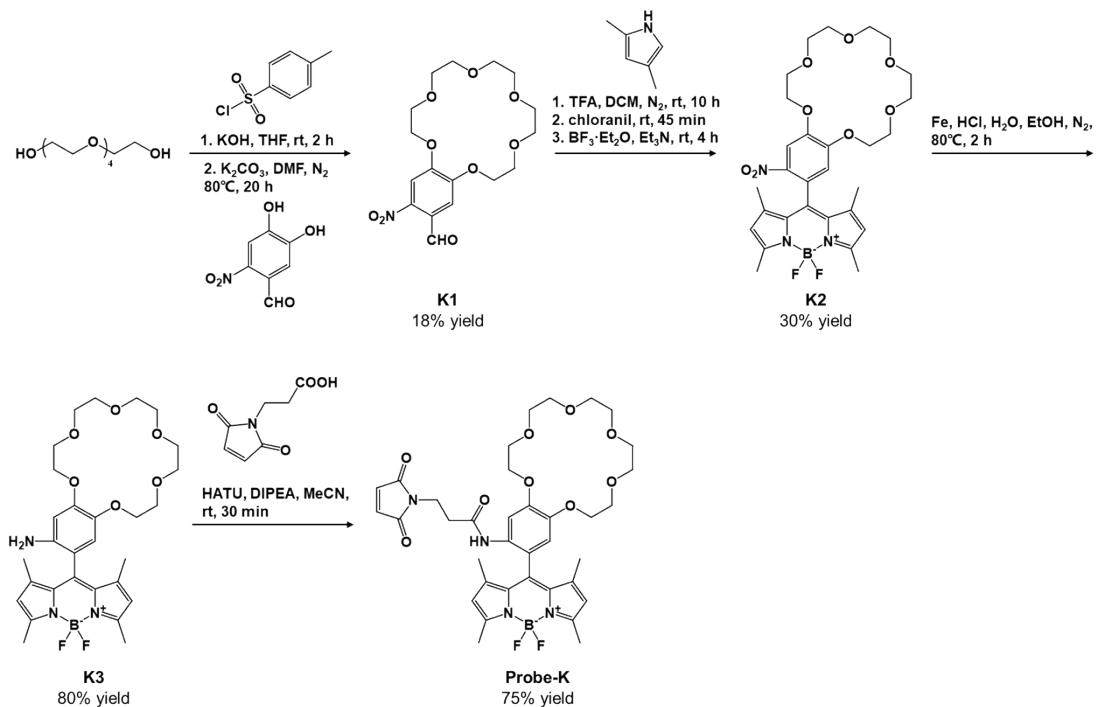
The images were obtained by an FV-1200 confocal laser scanning microscope with 60 $\times$ objective lens (cyan channel:  $\lambda_{ex} = 405$  nm,  $\lambda_{em} = 460$ -500 nm; green channel:

$\lambda_{\text{ex}} = 488 \text{ nm}$ ,  $\lambda_{\text{em}} = 520\text{-}560 \text{ nm}$ ; red channel:  $\lambda_{\text{ex}} = 559 \text{ nm}$ ,  $\lambda_{\text{em}} = 575\text{-}675 \text{ nm}$ ). The

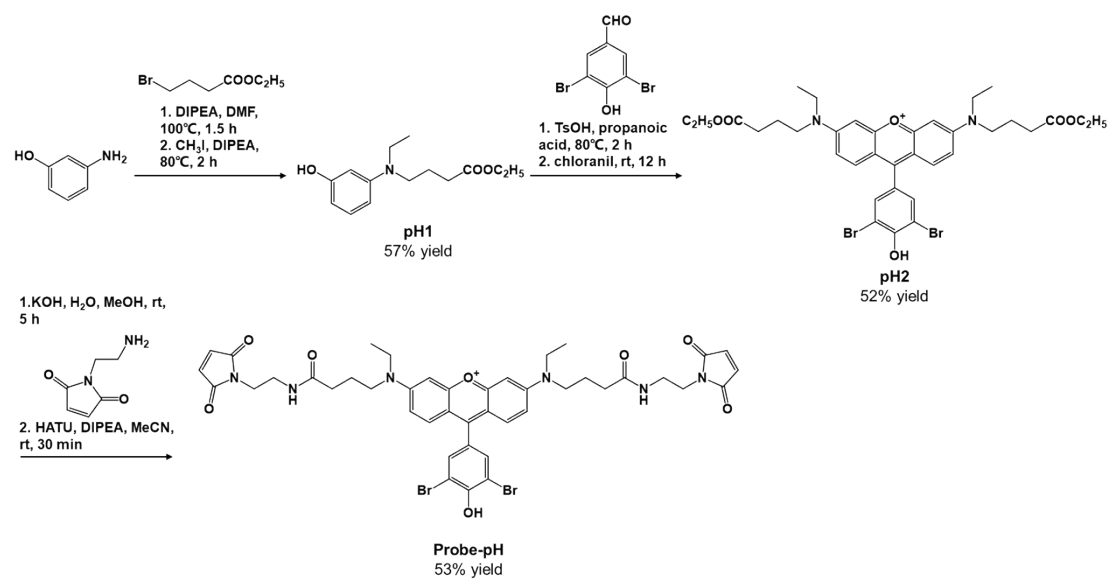
fluorescence optical density was calculated by image J software.



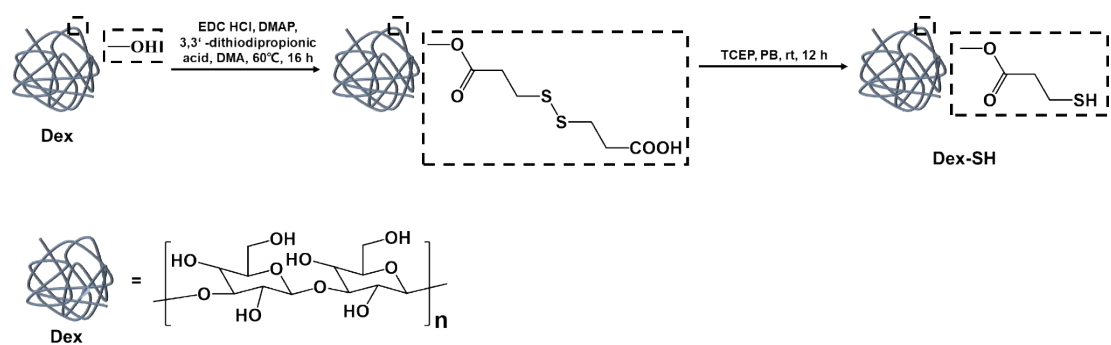
Scheme S1. The synthetic routes of Probe-C1.



Scheme S2. The synthetic routes of Probe-K.



Scheme S3. The synthetic routes of Probe-pH.



Scheme S4. The synthetic routes of sulfhydryl-functionalized dextran (Dex-SH).

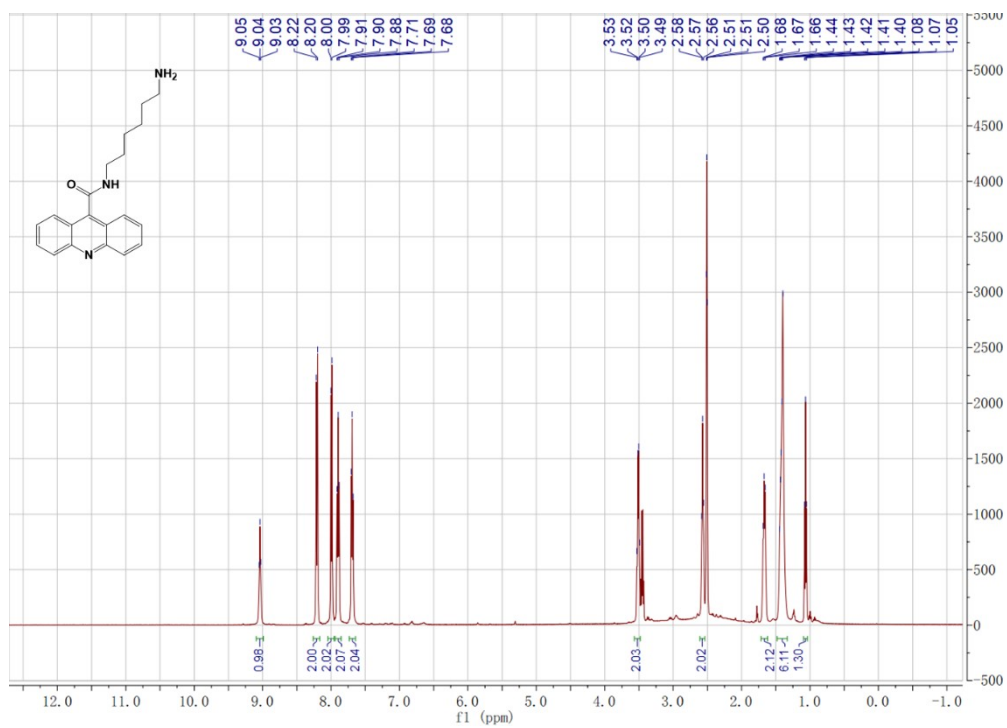


Fig. S1.  $^1\text{H}$  NMR spectrum of C11 in  $\text{DMSO-}d_6$ .

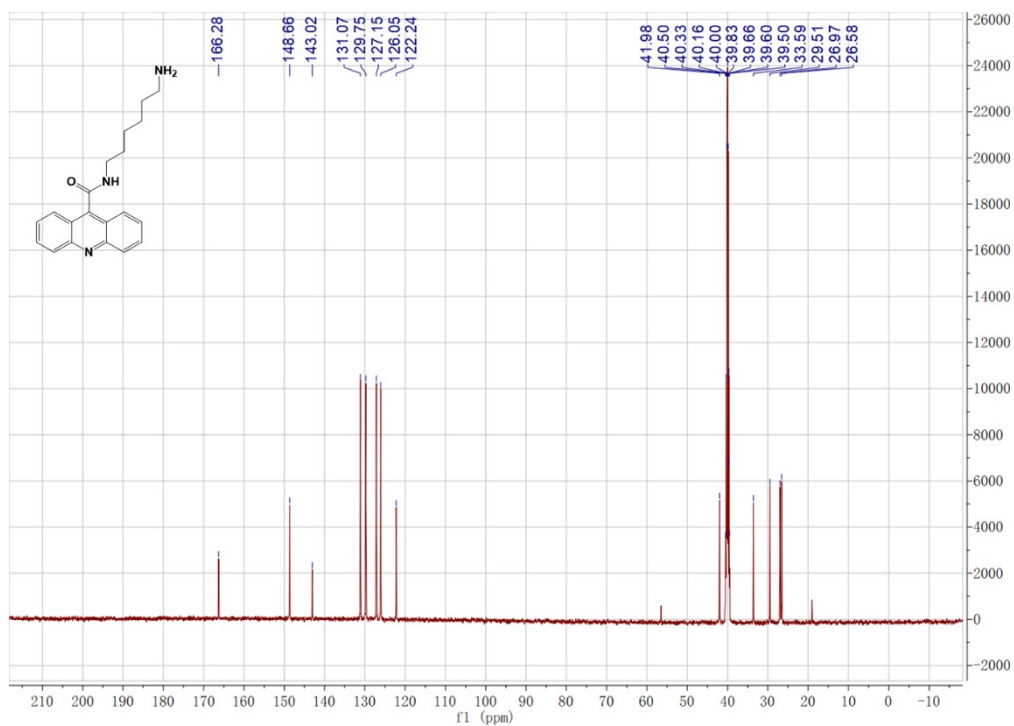


Fig. S2.  $^{13}\text{C}$  NMR spectrum of C11 in  $\text{DMSO-}d_6$ .

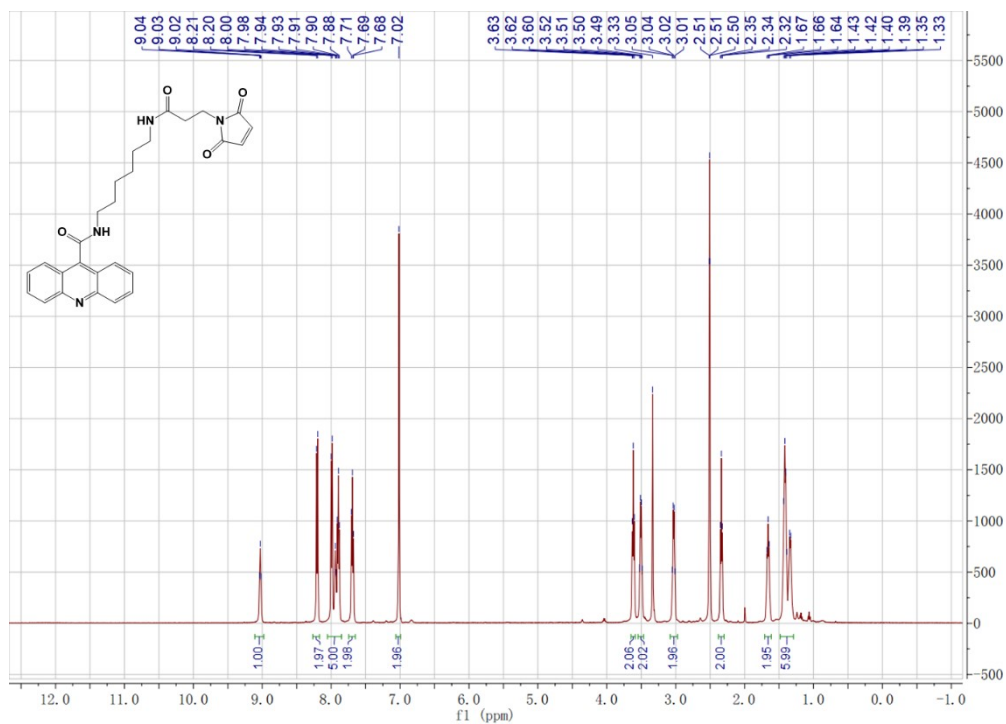


Fig. S3.  $^1\text{H}$  NMR spectrum of C12 in  $\text{DMSO-}d_6$ .

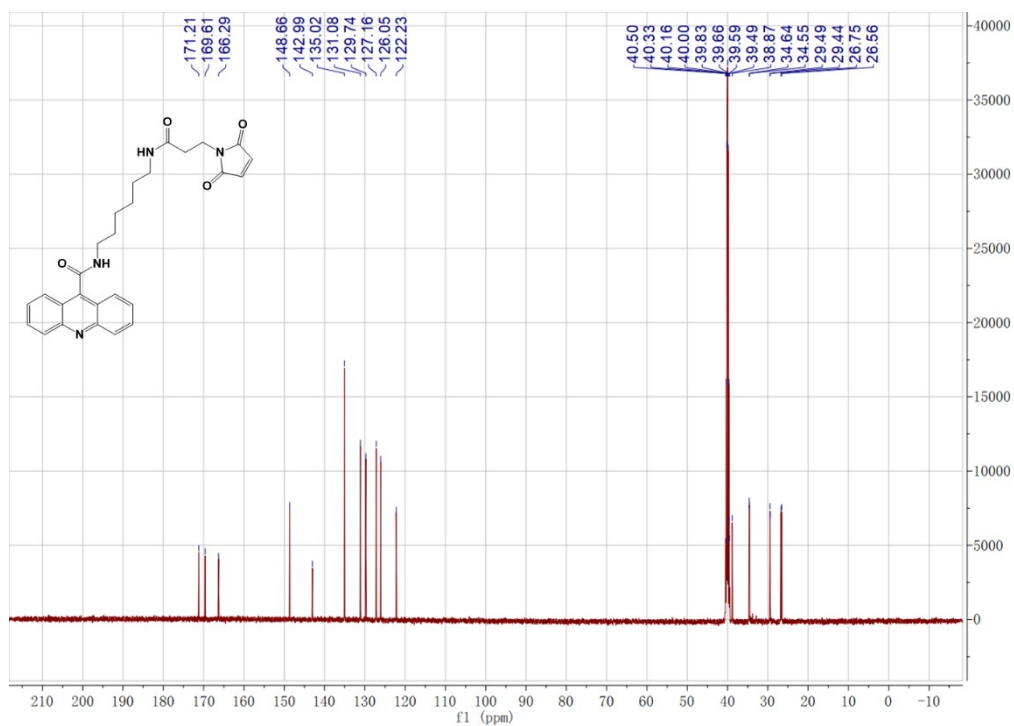


Fig. S4.  $^{13}\text{C}$  NMR spectrum of C12 in  $\text{DMSO-}d_6$ .



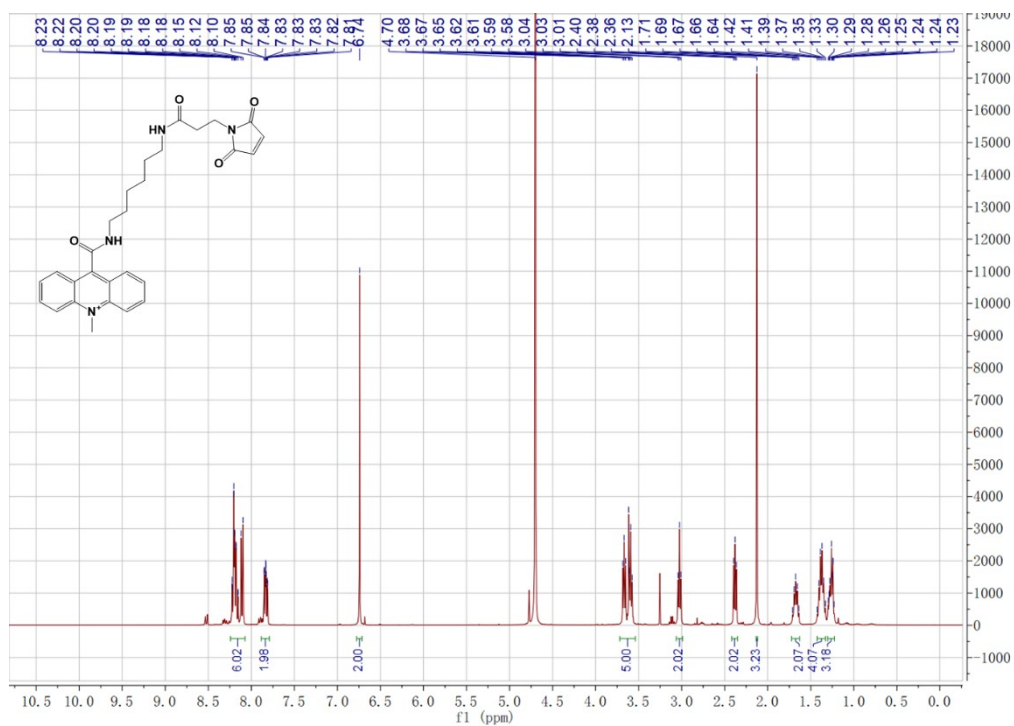


Fig. S5.  $^1\text{H}$  NMR spectrum of Probe-Cl in  $\text{D}_2\text{O}$ .

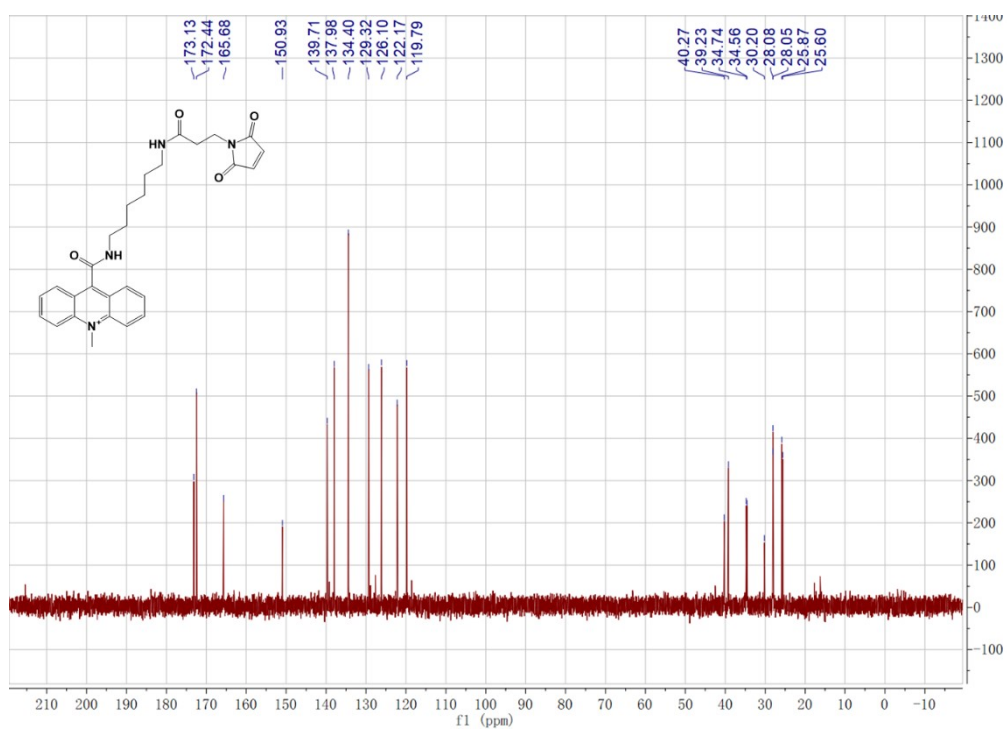


Fig. S6.  $^{13}\text{C}$  NMR spectrum of Probe-Cl in  $\text{D}_2\text{O}$ .

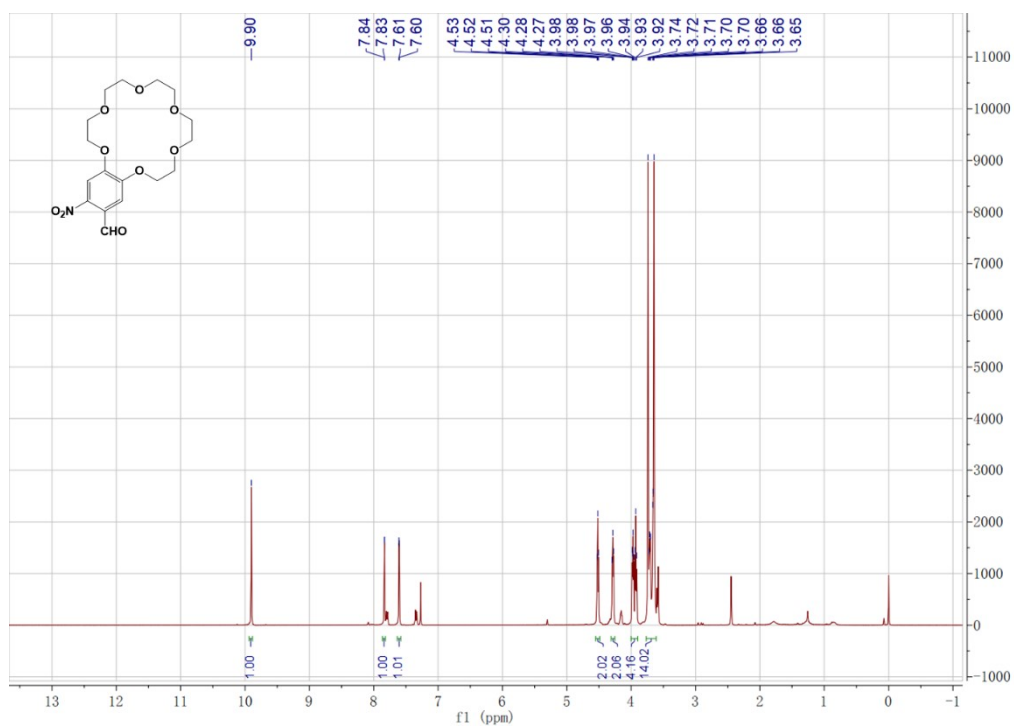


Fig. S7.  $^1\text{H}$  NMR spectrum of K1 in  $\text{CDCl}_3$ .

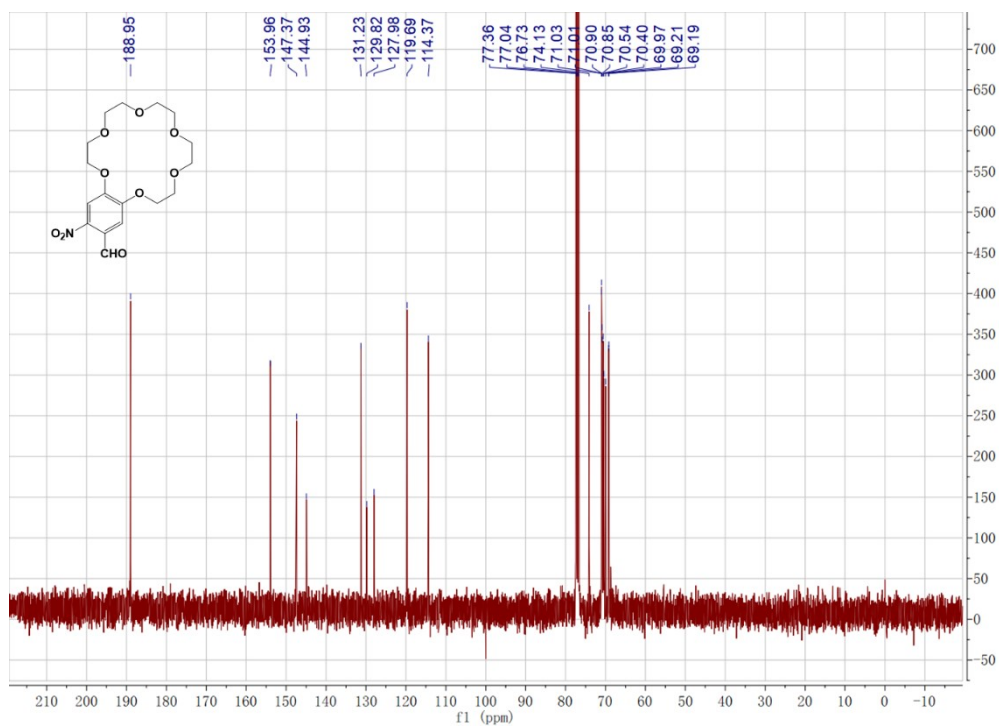


Fig. S8.  $^{13}\text{C}$  NMR spectrum of K1 in  $\text{CDCl}_3$ .

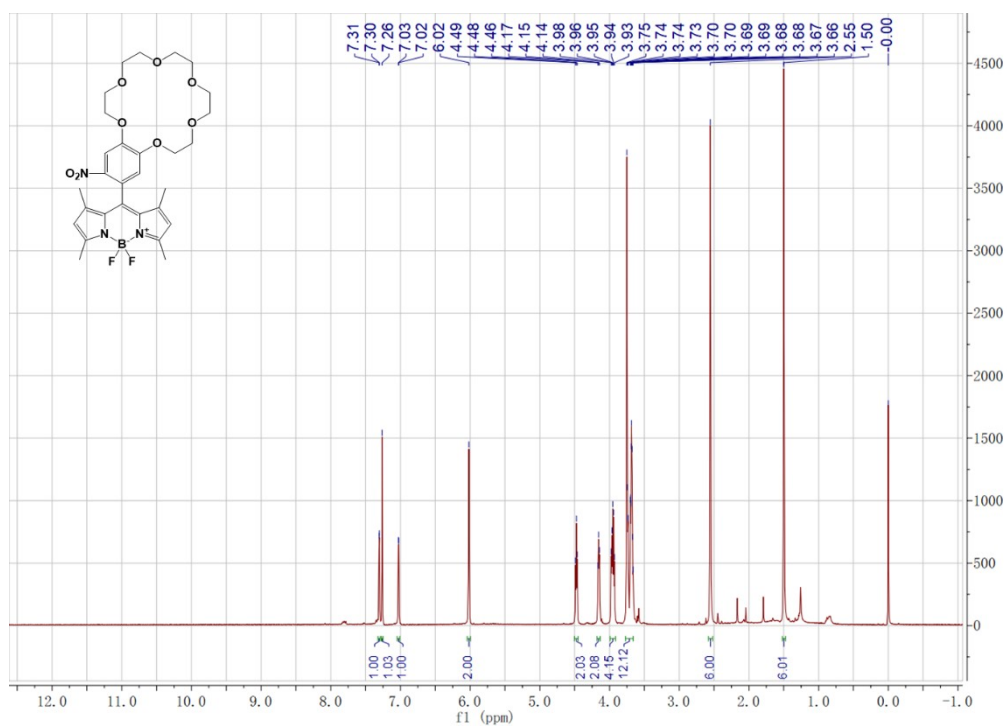


Fig. S9.  $^1\text{H}$  NMR spectrum of K2 in  $\text{CDCl}_3$ .

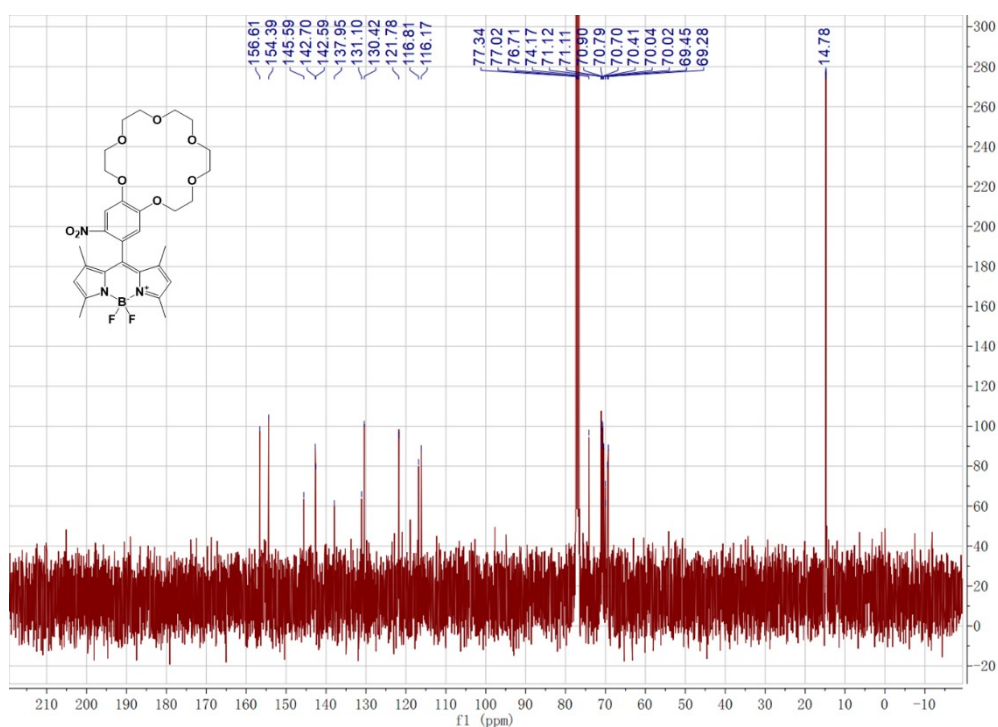


Fig. S10.  $^{13}\text{C}$  NMR spectrum of K2 in  $\text{CDCl}_3$ .

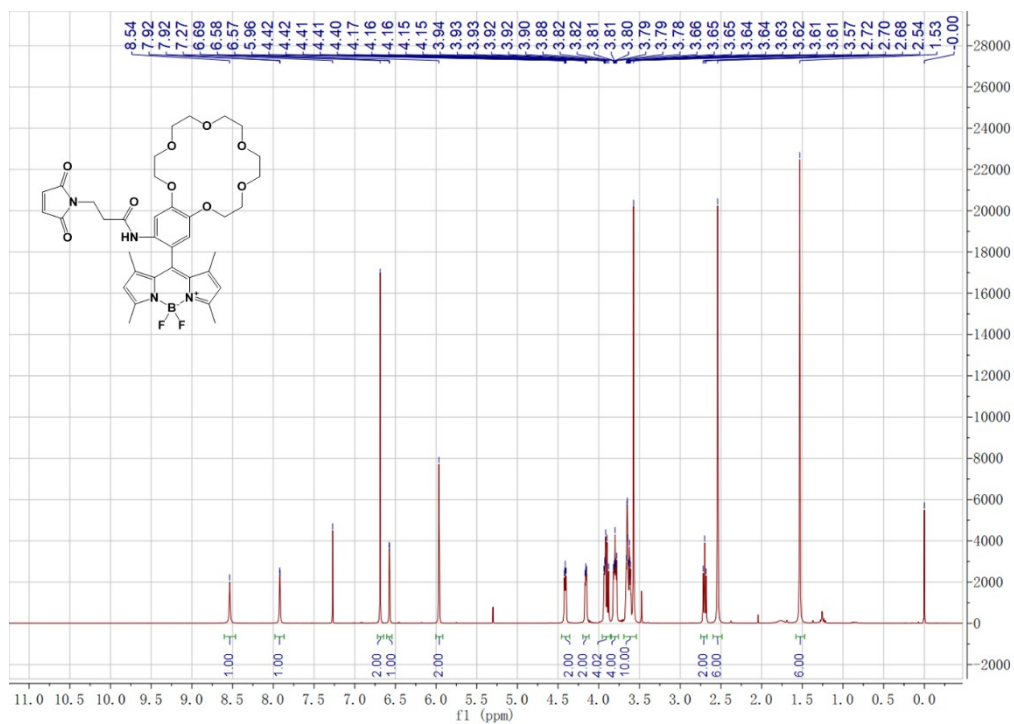


Fig. S11. <sup>1</sup>H NMR spectrum of Probe-K in CDCl<sub>3</sub>.

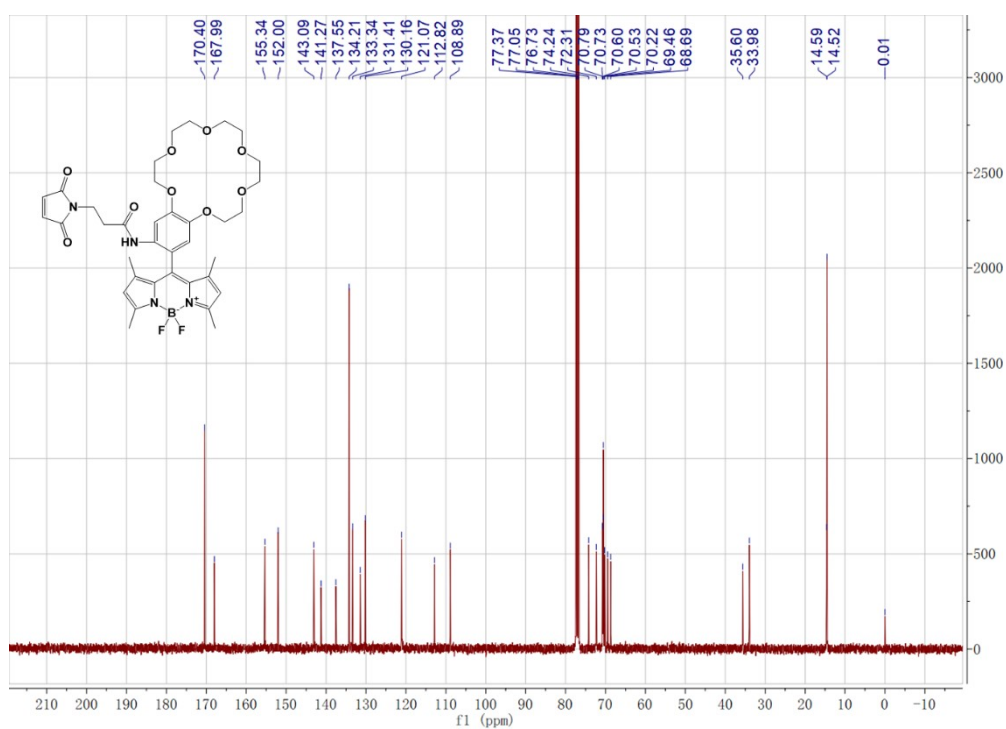


Fig. S12. <sup>13</sup>C NMR spectrum of Probe-K in CDCl<sub>3</sub>.

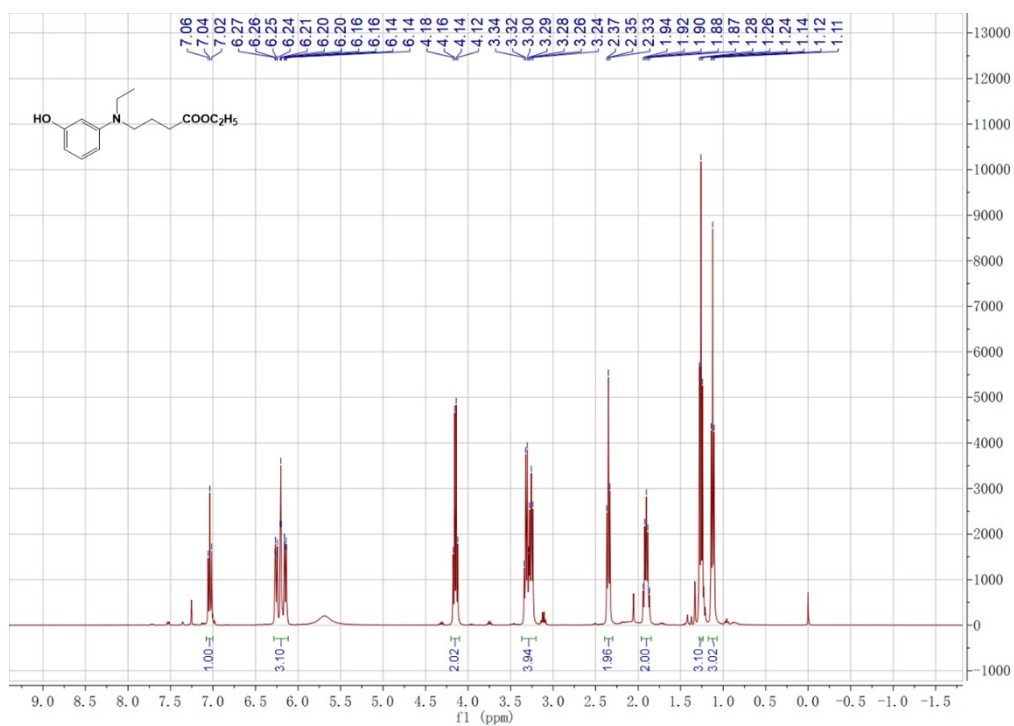


Fig. S13.  $^1\text{H}$  NMR spectrum of pH1 in  $\text{CDCl}_3$ .

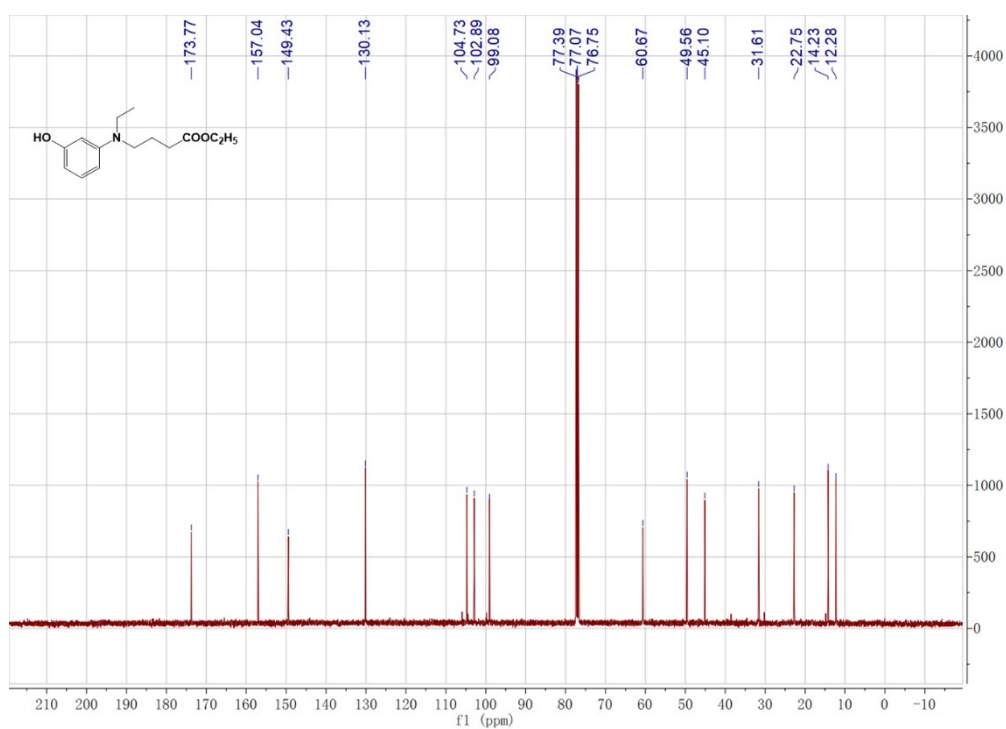


Fig. S14.  $^{13}\text{C}$  NMR spectrum of pH1 in  $\text{CDCl}_3$ .

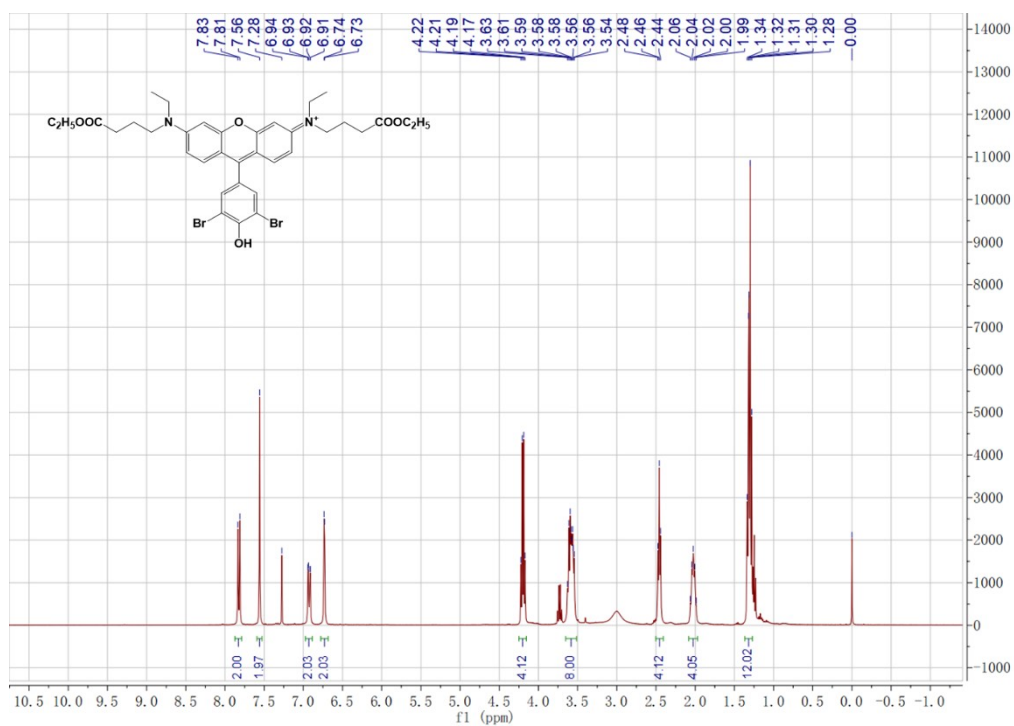


Fig. S15.  $^1\text{H}$  NMR spectrum of pH2 in  $\text{CDCl}_3$ .

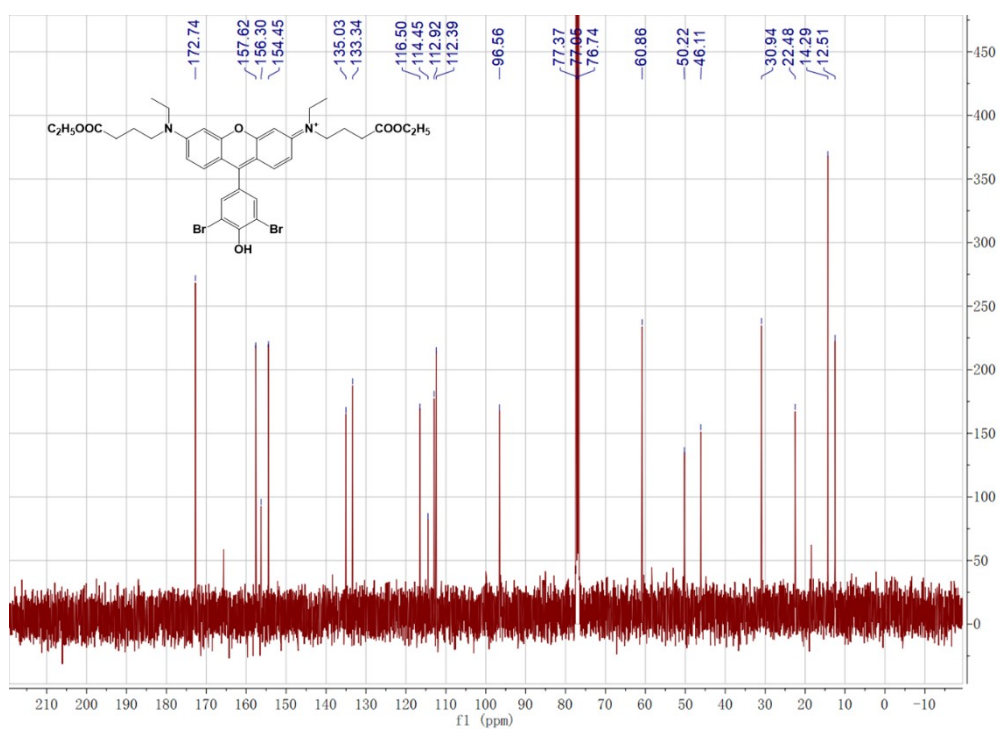


Fig. S16.  $^{13}\text{C}$  NMR spectrum of pH2 in  $\text{CDCl}_3$ .

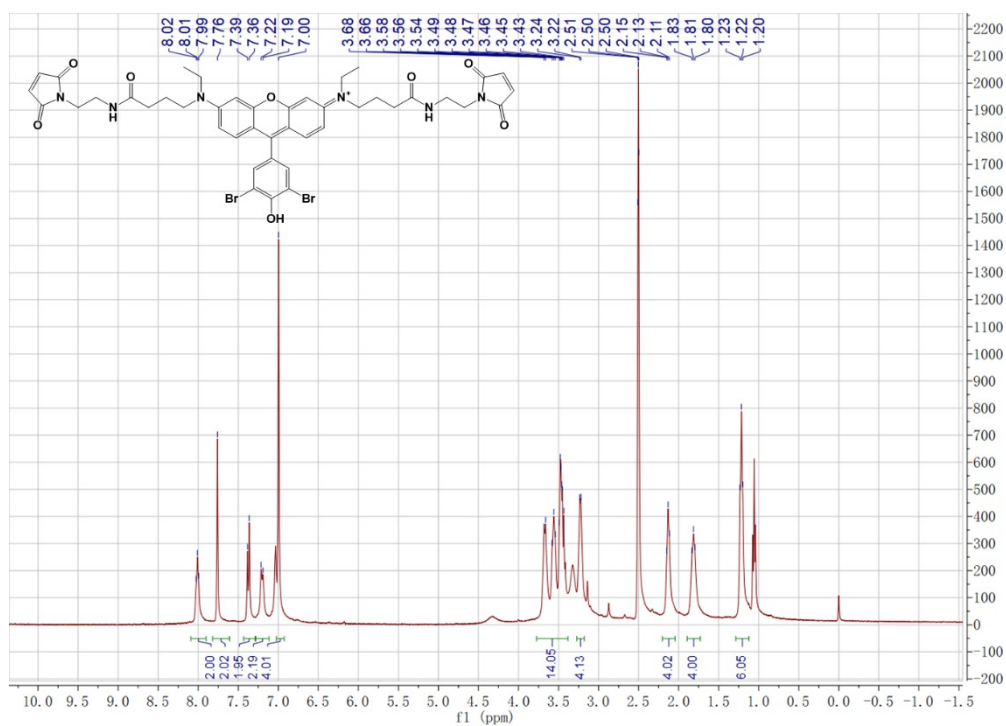


Fig. S17.  $^1\text{H}$  NMR spectrum of Probe-pH in  $\text{DMSO-}d_6$ .

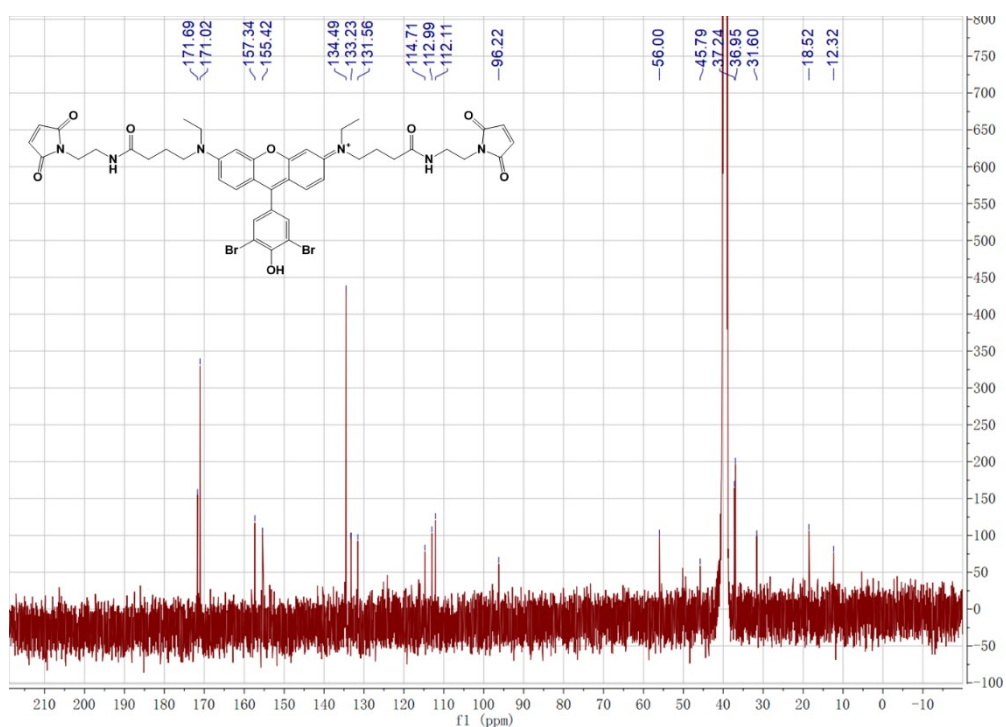


Fig. S18.  $^{13}\text{C}$  NMR spectrum of Probe-pH in  $\text{DMSO-}d_6$ .

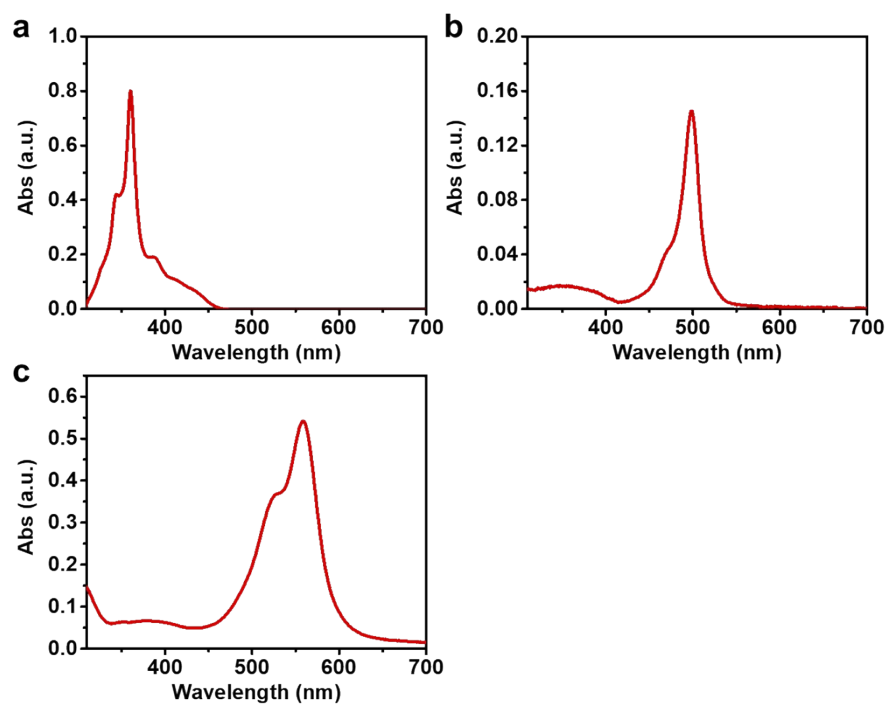


Fig. S19. Absorption spectra of (a) Probe-Cl (40  $\mu\text{M}$ ), (b) Probe-K (3  $\mu\text{M}$ ), and (c) Probe-pH (10  $\mu\text{M}$ ).



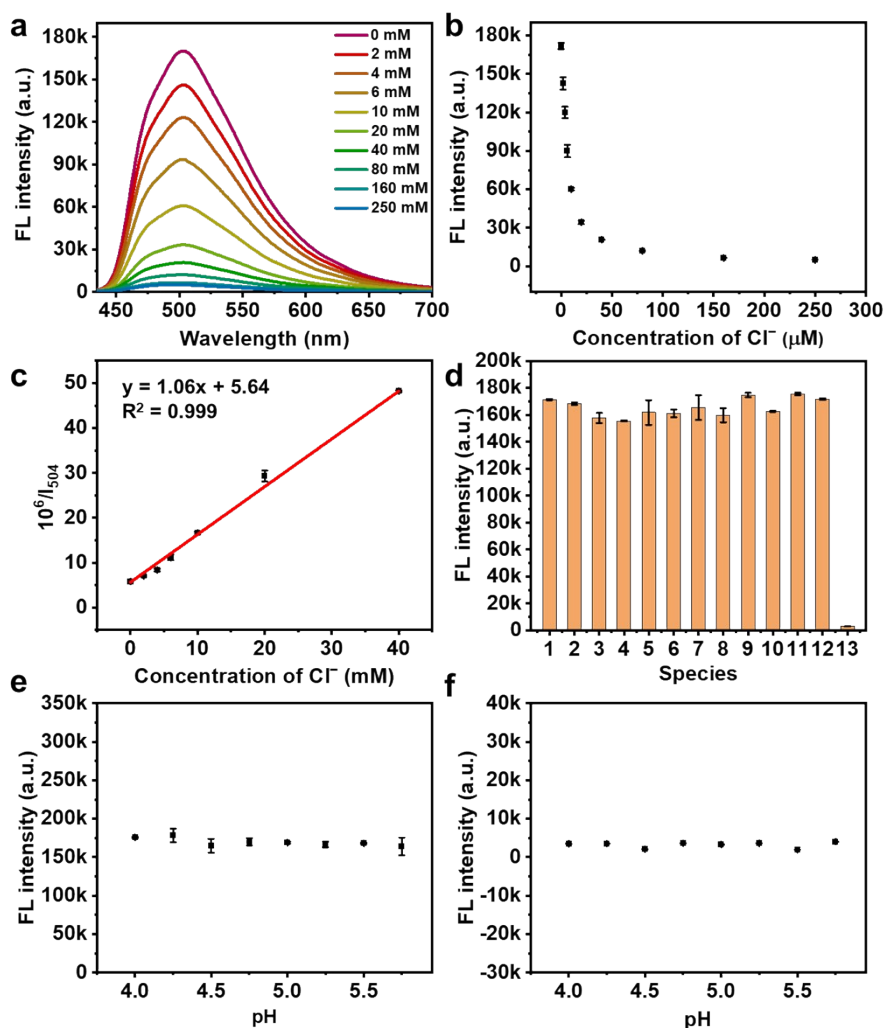


Fig. S20. (a) Fluorescence spectra of Probe-Cl at various  $\text{Cl}^-$  concentrations. (b) Reciprocal of fluorescence intensity at 504 nm of Probe-Cl ( $I_{504}$ ) in response to  $\text{Cl}^-$  at various concentrations. (c) The linear relationship between  $10^6/I_{504}$  and concentrations of  $\text{Cl}^-$ . (d) Fluorescence intensity at 504 nm upon the addition of various potential interfering species ((1. Blank, 2.  $\text{Ca}^{2+}$  (2 mM), 3.  $\text{K}^+$  (250 mM), 4.  $\text{Na}^+$  (250 mM), 5.  $\text{Mg}^{2+}$  (2 mM), 6.  $\text{Zn}^{2+}$  (2 mM), 7.  $\text{SO}_4^{2-}$  (2 mM), 8.  $\text{NO}_3^-$  (2 mM), 9.  $\text{Br}^-$  (50  $\mu\text{M}$ ), 10.  $\text{F}^-$  (100  $\mu\text{M}$ ), 11.  $\text{Fe}^{2+}$  (2 mM), 12.  $\text{I}^-$  (50  $\mu\text{M}$ ), 13.  $\text{Cl}^-$  (250 mM)). (e) Fluorescence intensity at 504 nm of Probe-Cl at different pH without  $\text{Cl}^-$ . (f) Fluorescence intensity at 504 nm of Probe-Cl at different pH in the presence of 250 mM  $\text{Cl}^-$ .

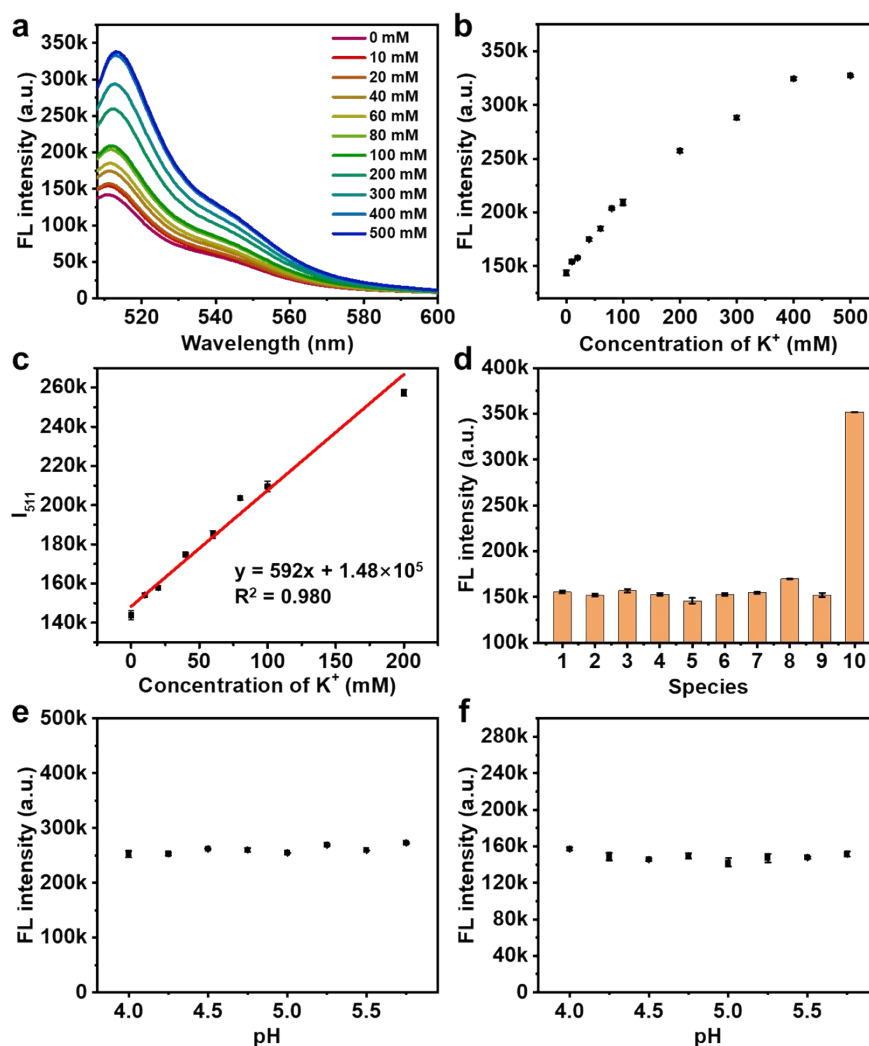


Fig. S21. (a) Fluorescence spectra of Probe-K at various K<sup>+</sup> concentrations. (b) Reciprocal of fluorescence intensity at 511 nm of Probe-K ( $I_{511}$ ) in response to K<sup>+</sup> at various concentrations. (c) The linear relationship between  $I_{511}$  and concentrations of K<sup>+</sup>. (d) Fluorescence intensity at 511 nm upon the addition of various potential interfering species (1. Blank, 2. Al<sup>3+</sup> (100  $\mu$ M), 3. Ca<sup>2+</sup> (2 mM), 4. Cu<sup>2+</sup> (100  $\mu$ M), 5. Fe<sup>3+</sup> (100  $\mu$ M), 6. Mg<sup>2+</sup> (2 mM), 7. Mn<sup>2+</sup> (1 mM), 8. Na<sup>+</sup> (250 mM), 9. Zn<sup>2+</sup> (2 mM), 10. K<sup>+</sup> (250 mM)). (e) Fluorescence intensity at 511 nm of Probe-K at different pH in the presence of 200 mM K<sup>+</sup>. (f) Fluorescence intensity at 504 nm of Probe-K at different pH without K<sup>+</sup>.

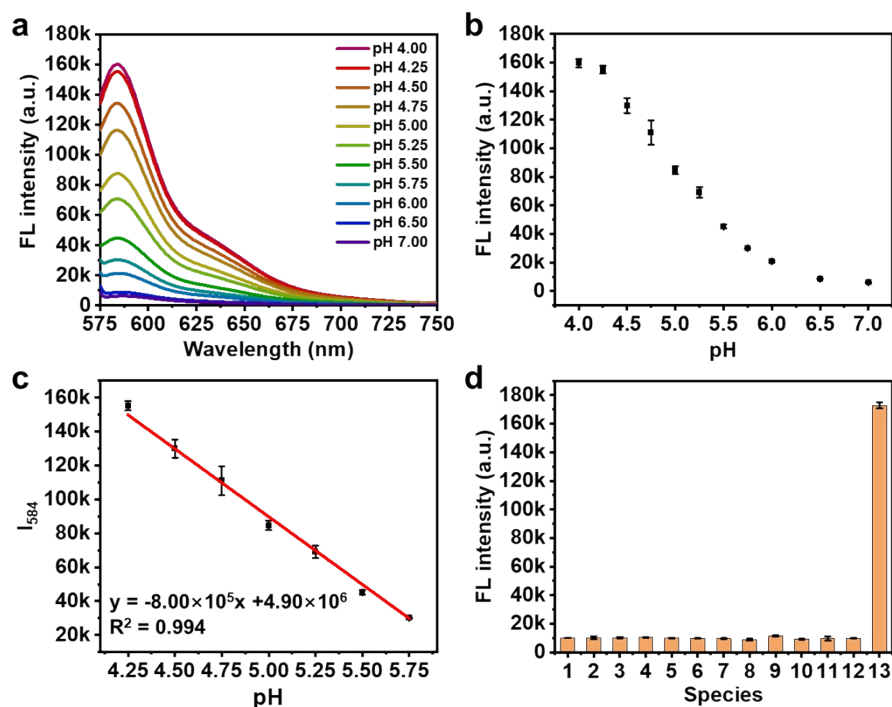


Fig. S22. (a) Fluorescence spectra of Probe-pH at various pH. (b) Response of reciprocal of fluorescence intensity at 584 nm of Probe-pH ( $I_{584}$ ) to various pH. (c) The linear relationship between  $I_{584}$  and pH. (d) Fluorescence intensity at 584 nm upon the addition of various potential interfering species (1. Blank, 2.  $\text{Br}^-$  (100  $\mu\text{M}$ ), 3.  $\text{Ca}^{2+}$  (100  $\mu\text{M}$ ), 4.  $\text{Cl}^-$  (250 mM), 5.  $\text{F}^-$  (100  $\mu\text{M}$ ), 6.  $\text{Fe}^{3+}$  (100  $\mu\text{M}$ ), 7.  $\text{I}^-$  (100  $\mu\text{M}$ ), 8.  $\text{Mg}^{2+}$  (100  $\mu\text{M}$ ), 9.  $\text{Na}^+$  (250 mM), 10.  $\text{NO}_3^-$  (2 mM), 11.  $\text{SO}_4^{2-}$  (2 mM), 12.  $\text{Zn}^{2+}$  (100  $\mu\text{M}$ ), 13. pH = 4.00). The pH of species 1-12 is 7.00.

Under 405 nm excitation, the fluorescence intensity of Probe-Cl decreased gradually with the increase of  $[\text{Cl}^-]$  in 0-160 mM (Fig. S19a). The reciprocal of fluorescence intensity at 504 nm was linearly correlated with  $[\text{Cl}^-]$  in 0-40 mM ( $y = 4.06x + 5.64$ ,  $R^2 = 0.999$ , where  $y$  is  $10^6/I_{504}$ ), with a detection limit of 0.24 mM (Fig. S19b and c). Probe-Cl showed satisfactory selectivity (Fig. S19d). As shown in Fig.

S19e and f, the pH did not affect Probe-Cl signal whether  $\text{Cl}^-$  presence or absence, indicating the pH-independent of Probe-Cl. Under 488 nm excitation, the fluorescence intensity of Probe-K gradually increased with the increase of  $[\text{K}^+]$  in 0-400 mM (Fig. 20a). The fluorescence intensity at 511 nm was linearly correlated with  $[\text{K}^+]$  in 0-200 mM ( $y = 592x + 1.48 \times 10^5$ ,  $R^2 = 0.980$ ), and the detection limit was 1.9 mM (Fig. S20b and c). The satisfactory selectivity and pH-independent of Probe-K was verified in Figure S20d-f. Under 559 nm excitation, the fluorescence intensity of Probe-pH gradually decreased with the increase of pH in 4.00-6.50. The fluorescence intensity at 584 nm was linearly correlated with pH in 4.25-5.75 ( $y = -8.00 \times 10^5x + 4.90 \times 10^6$ ,  $R^2 = 0.994$ ) (Fig. S21b and c). The selectivity Probe-pH was verified in Figure S21d.

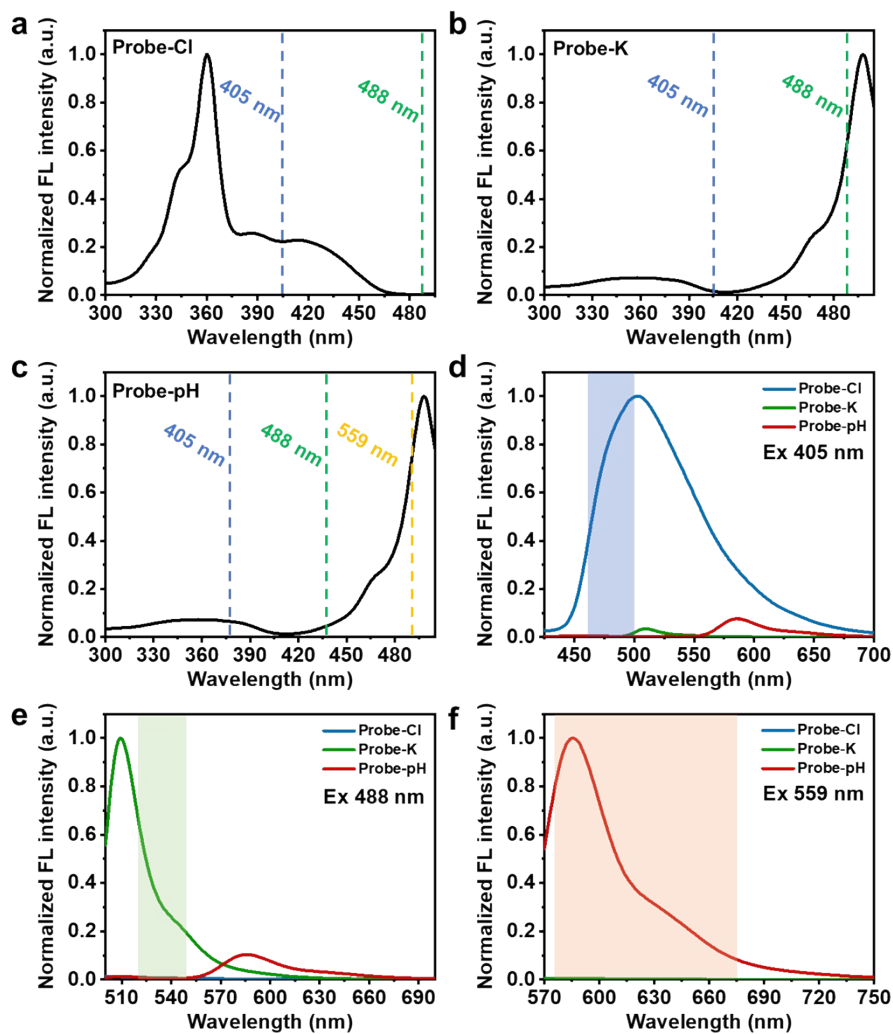


Fig. S23. (a) The excitation spectrum of Probe-Cl. (b) The excitation spectrum of Probe-K. (c) The excitation spectrum of Probe-pH. Superimposed emission spectra of Probe-Cl, Probe-K, and Probe-pH excited at (d) 405, (e) 488, and (f) 559 nm, respectively.

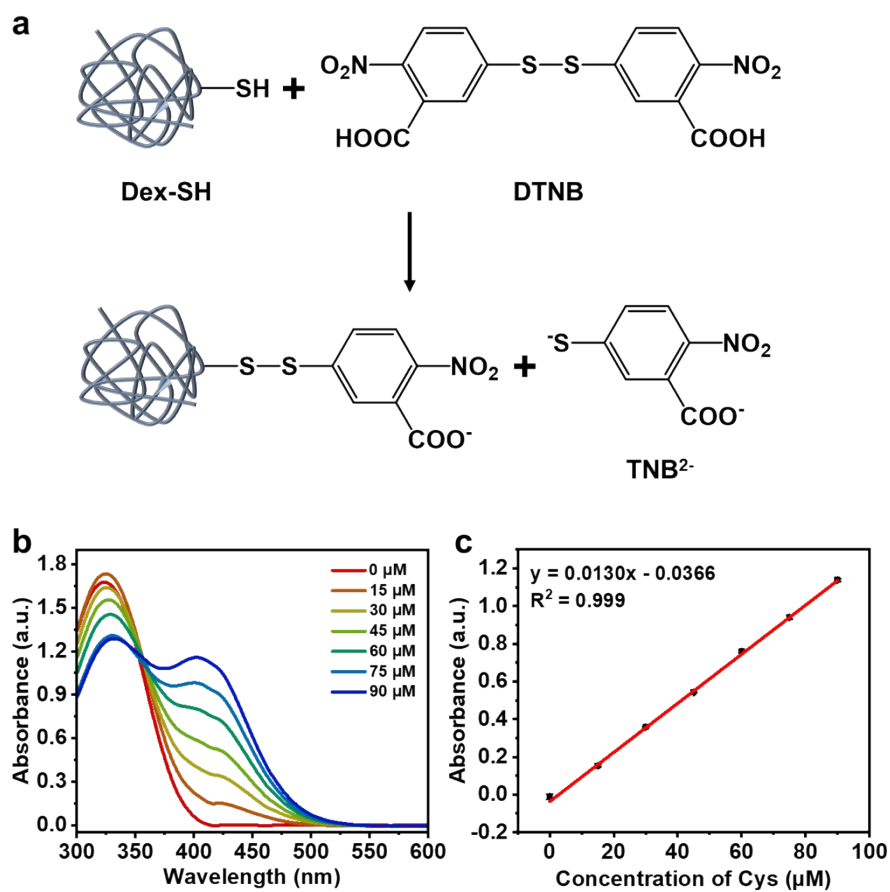


Fig. S24. (a) Detection mechanism of -SH. (b) Absorption spectra of DTNB solution in the presence of different concentrations of cysteine. (c) Linear relationship between the absorbance at 412 nm and cysteine concentration.

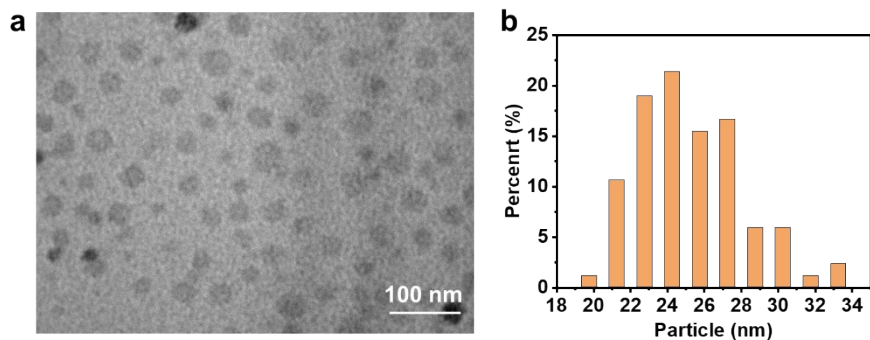


Fig. S25. (a) TEM image of TR-probe and (b) particle size statistics.

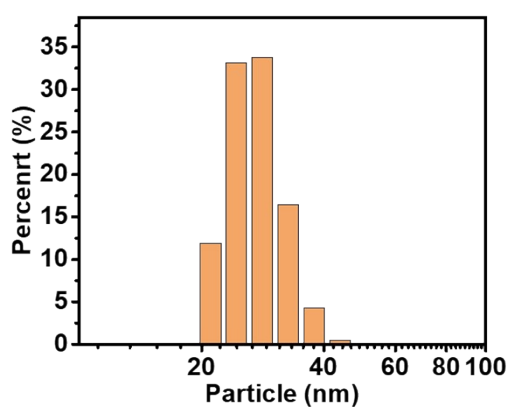


Fig. S26. Particle size of TR-probe from dynamic light scattering.

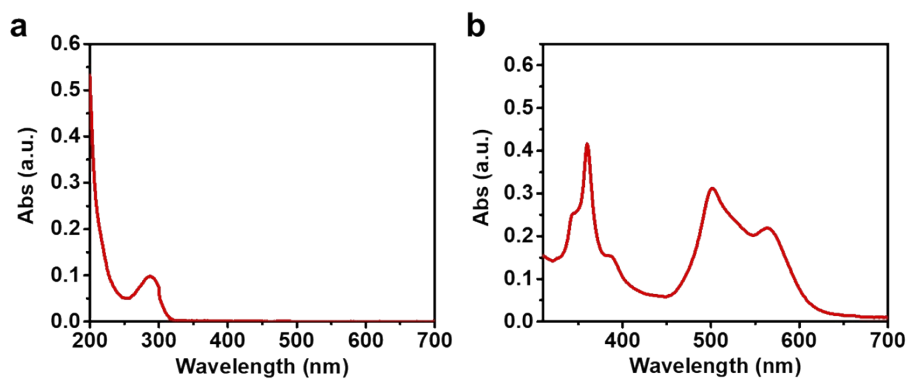


Fig. S27. Absorption spectra of (a) Dex-SH ( $100 \mu\text{g mL}^{-1}$ ) and (b) TR-probe ( $50 \mu\text{g mL}^{-1}$ ).

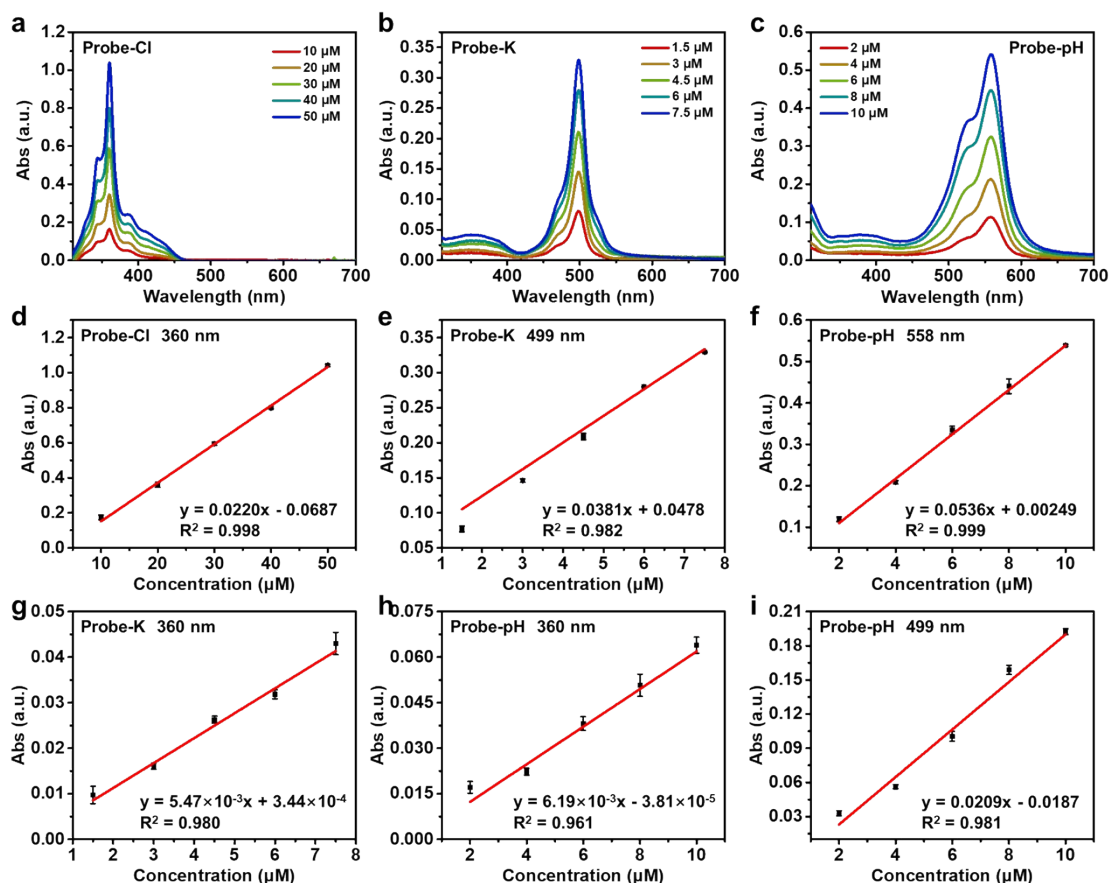


Fig. S28. Absorption spectra of different concentrations (a) Probe-Cl, (b) Probe-K, and (c) Probe-pH solution. (d) Linear relationship between the absorbance of Probe-Cl at 360 nm and concentration. (e) Linear relationship between the absorbance of Probe-K at 449 nm and concentration. (f) Linear relationship between the absorbance of Probe-pH at 558 nm and concentration. (g) Linear relationship between the absorbance of Probe-K at 360 nm and concentration. (h) Linear relationship between the absorbance of Probe-pH at 360 nm and concentration. (i) Linear relationship between the absorbance of Probe-pH at 449 nm and concentration.

The loading amounts of Probe-Cl, Probe-K, and Probe-pH were calculated by absorption spectra (Fig. S28). Dex-SH has no absorption above 310 nm, and TR-probe



has absorption bands from Probe-Cl, Probe-K, and Probe-pH (Fig. S27). Only Probe-pH has absorption at 558 nm, the loading amount of Probe-pH can be calculated by the absorbance at 558 nm. Probe-pH and Probe-K have absorption at 499 nm. After calculating the concentration of Probe-pH, its absorbance at 499 nm can be obtained. The total absorbance minus the absorbance from Probe-pH gives the absorbance from Probe-K at 499 nm, further calculating the loading amount of Probe-K. The absorption at 360 nm was from Probe-Cl, Probe-K, and Probe-pH. The loading amount of Probe-Cl can be calculated by subtracting the absorbance from Probe-K and Probe-pH at 360 nm in a similar way. The loading amounts of Probe-Cl, Probe-K, and Probe-pH in TR-probe were 0.079, 0.10, and 0.38 mmol g<sup>-1</sup>, respectively.

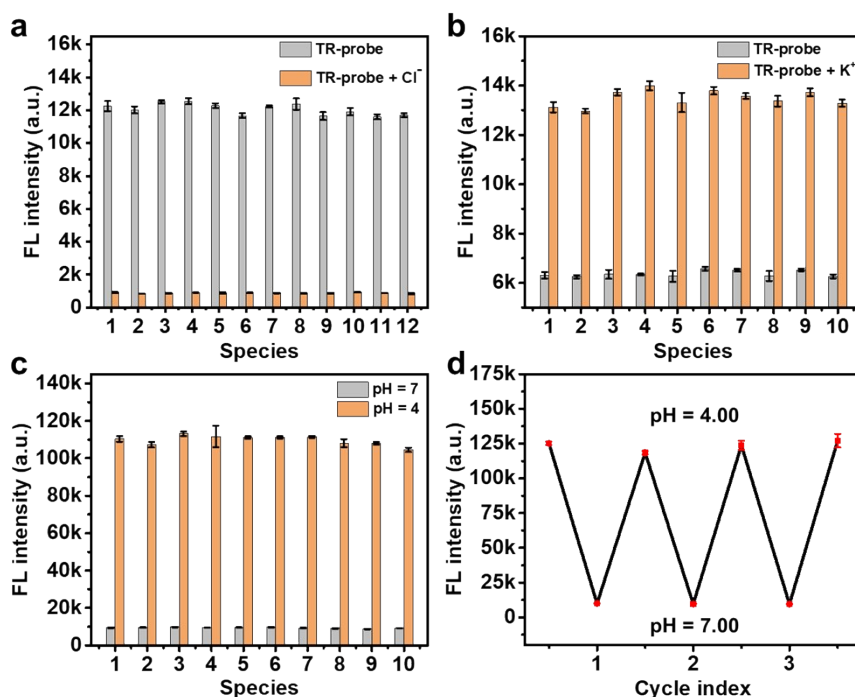


Fig. S29. (a) Fluorescence intensity ( $\lambda_{\text{ex}} = 405 \text{ nm}$ ,  $\lambda_{\text{em}} = 504 \text{ nm}$ ) of TR-probe upon the addition of different potential interfering species (1. Blank, 2.  $\text{Ca}^{2+}$  (2 mM), 3.  $\text{Fe}^{2+}$  (2 mM), 4.  $\text{Mg}^{2+}$  (2 mM), 5.  $\text{Na}^+$  (250 mM), 6.  $\text{F}^-$  (100  $\mu\text{M}$ ), 7.  $\text{NO}_3^-$  (2 mM), 8.  $\text{SO}_4^{2-}$  (2 mM), 9.  $\text{Br}^-$  (50  $\mu\text{M}$ ), 10.  $\text{I}^-$  (50  $\mu\text{M}$ ), 11.  $\text{Zn}^{2+}$  (2 mM), 12. mixture) when  $\text{Cl}^-$  (250 mM) is present or absent. (b) Fluorescence intensity ( $\lambda_{\text{ex}} = 488 \text{ nm}$ ,  $\lambda_{\text{em}} = 510 \text{ nm}$ ) of TR-probe upon the addition of different potential interfering species (1. Blank, 2.  $\text{Al}^{3+}$  (100  $\mu\text{M}$ ), 3.  $\text{Ca}^{2+}$  (2 mM), 4.  $\text{Cu}^{2+}$  (100  $\mu\text{M}$ ), 5.  $\text{Fe}^{3+}$  (100  $\mu\text{M}$ ), 6.  $\text{Mg}^{2+}$  (2 mM), 7.  $\text{Mn}^{2+}$  (1 mM), 8.  $\text{Zn}^{2+}$  (2 mM), 9.  $\text{Na}^+$  (250 mM), 10. mixture) when  $\text{K}^+$  (300 mM) is present or absent. (c) Fluorescence intensity ( $\lambda_{\text{ex}} = 559 \text{ nm}$ ,  $\lambda_{\text{em}} = 591 \text{ nm}$ ) of TR-probe upon the addition of different potential interfering species (1. Blank, 2.  $\text{Br}^-$  (100  $\mu\text{M}$ ), 3.  $\text{Cl}^-$  (250 mM), 4.  $\text{F}^-$  (100  $\mu\text{M}$ ), 5.  $\text{Fe}^{3+}$  (100  $\mu\text{M}$ ), 6.  $\text{I}^-$  (100  $\mu\text{M}$ ), 7.  $\text{Na}^+$  (250 mM), 8.  $\text{NO}_3^-$  (2 mM), 9.  $\text{SO}_4^{2-}$  (2 mM), 10. mixture) when pH = 4.00 or 7.00. (d) Fluorescence reversibility of TR-probe ( $\lambda_{\text{ex}} = 559 \text{ nm}$ ,  $\lambda_{\text{em}} = 591 \text{ nm}$ ) against pH change between 4.00 and 7.00.

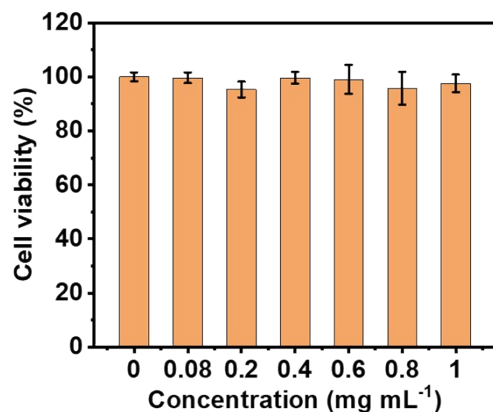


Fig. S30. Cytotoxicity of different concentrations of TR-probes on A549 cells.

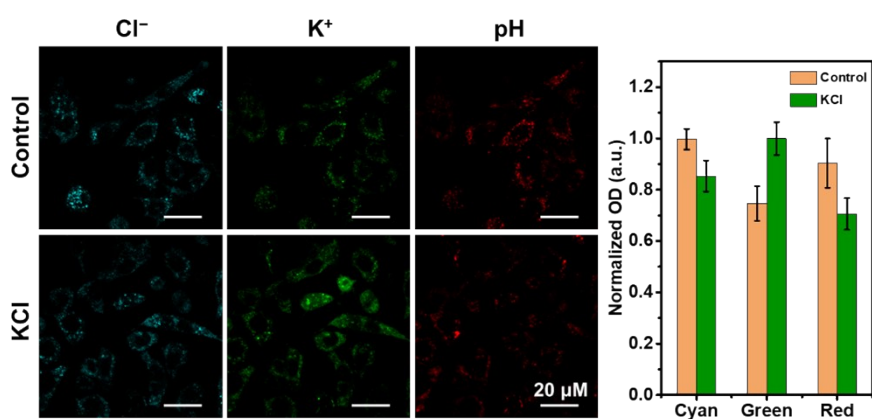


Fig. S31. CLSM images and corresponding normalized optical density of TR-probe stained 549 cells treated with 200 mM KCl for 3 h.

## References

- [1] N. Wang, X. Yu, T. Deng, K. Zhang, R. Yang and J. Li, *Anal. Chem.*, 2020, **92**, 583-587.
- [2] K. Leung, K. Chakraborty, A. Saminathan and Y. Krishnan, *Nat. Nanotechnol.*, 2019, **14**, 176-183.
- [3] P. Anees, A. Saminathan, E. R. Rozmus, A. Di, A. B. Malik, B. P. Delisle and Y. Krishnan, *Nat. Biotechnol.*, 2023, <https://doi.org/10.1038/s41587-023-01928-z>.